Fabrication and characterization of
AlGaN/GaN High Electron Mobility Transistors (HEMT)

by

Chungman Yang

A dissertation submitted to the Graduate Faculty of
Auburn University
in partial fulfillment of the
requirements for the Degree of
Master of Science

Auburn, Alabama
May 9, 2015

Key words: HEMT, GaN, Photocurrent,
breakdown, fabrication, characterization

Approved by

Minseo Park, Chair, Professor of Physics
Jianjun Dong, Professor of Physics
Ayayi Claude Ahyi, Associate Research Professor of Physics

Abstract

As primary material for semiconductor fabrication field, Gallium nitride has attracted lots of interest of scientists and developers due to its unique and exceptional electrical properties such as high thermal conductivity, high electron mobility, high breakdown field, and mechanical and chemical endurance under harsh conditions. Since GaN has those superior electrical properties induced by its wide band gap energy compared to the conventional semiconductor materials, it would be applied to many different electronic applications. This dissertation describes the fabrication and characterization of high electron mobility transistor(HEMT) based on GaN wafer. The HEMTs consist of the schottky metal contact and ohmic contact on same direction of the wafer. A GaN layer has been deposited on the silicon wafer. Between gallium nitride layer and the silicon substrate there are different layers to buffer each layers. The ohmic contact will be connected by electron channel through the GaN layers where the two- dimensional electron gas channel (2DEG) is formed. Two dimensional electron gas channel would allow electron carriers to pass through without any intentional dopings, which makes costs less and reduced processing steps to fabricate. Fabricated HEMTs are characterized by measuring current-voltage curve (I-V) and capacitance-voltage curve (C-V), in order to verify HEMT's electrical properties. Photocurrent-voltage curve measurement also has been carried out to investigate how the GaN would react to light illumination and how the electric current output could increase.

Acknowledgement

I would like to express the deepest appreciation to Dr. Minseo Park for his precious dedication, advice, and encouragement to guide me during my graduate studying in Auburn University and letting me have enjoyable thesis work with continuous comments and suggestions. The author also is appreciate to Dr. Jianjun Dong, and Dr. Ayayi Claude Ahyi for their advice whenever I have a concerns and problems.

I also wish to thank to Dr. Jianjun Dong and Dr. Ayayi Claude Ahyi for their advice to hold me up for consistent work during studying in Auburn and also serving as committee members even at hardship.

I would like to thank to Dr. Ayayi Claude Ahyi, Dr. Resham Thapa, Dr. Yogesh Sharma, Dr. Tong Fei, and Ms. Tamara F Isaacs-Smith for training me on the semiconductor process system so that I could get used to the systems and complete my experiment.

Also, I would like to thanks Ms. Burcu Ozden, and Mr. Vahid Mirkhani for their cooperation with me on the device measurement and preparation and priceless advices. I would like to thanks to Mr. Kevin G Ross, Mr. Mohamad Menati, Mr. Collin R Wade, and Mr. Sunil Uprety for invaluable support and encouragement as peers.

In addition I would like to thank my family, Mr. Dongjo Yang, Ms. Samsoon Oh, Ms. Sehee Yang, Mr. Jungho Noh and Ms. Eunji Lee. The words cannot express their endless supports and love.

Table of Contents

Abstract ii

Acknowledgments iii

List of Tables vi

List of Figures vii

List of Abbreviations ix

Chapter 1 Introduction and Background 1

1.1 Introduction 1

1.2 Ohmic contacts 11

1.3 Schottky contacts 13

Chapter 2 Device Fabrication 15

2.1 Introduction 15

2.2 AlGaN/GaN wafer preparation 15

2.3 Cleaning 16

2.4 Photo-Lithography 18

2.5 Metallization 22

2.6 Rapid Thermal Annealing (RTA) 24

2.7 Summary 27

Chapter 3 Device Characterization 28

3.1 Introduction 28

3.2 Current-Voltage measurement 28

3.3 Capacitance-Voltage measurement 32

3.3 Summary 35

Chapter 4 Photo Current Voltage Measurement of AlGaN/GaN HEMT 36

4.1 Introduction 36

4.2 Current collapse 37

4.3 Photoionization 38

4.4 Experiment and Photocurrent measurement 39

4.5 Results and discussions 43

4.6 Summary and conclusions 46

Chapter 5 Breakdown Voltage Measurement and Analysis 47

5.1 Introduction 47

5.2 Breakdown phenomenon and measurement 48

5.3 Conclusions 53

References 54

List of Tables

Table 1.1 Breakdown fields, band gap energies, and dielectric constants for various semiconductor materials 3

Table 5.1 Breakdown measurement with different sizes and sweeping directions 51

List of Figures

Figure 1.1 Wurtzite and Zincblende structures of GaN 2

Figure 1.2 PL spectra of different temperature and x composition of $Al_xGa_{1-x}N$ 4

Figure 1.3 AlGaN/GaN based HEMT structue 5

Figure 1.4 Band structure of AlGaN/GaN based HEMT 6

Figure 1.5 (a) Individual polarization charge contributions (b) Polarization induced net charge (c) the AlGaN/GaN HEMT with polarization induced net charge and surface charge contributions 7

Figure 1.6 Contributions to electron mobility of different mechanisms in GaN 8

Figure 1.7 A sketch of FET I–V characteristics before (full curves) and after (dotted curves) current collapse. The maximum attainable device output power is approximately proportional to the area of the shaded and broken rectangles, before and after collapse, respectively 9

Figure 1.8 Reactions among different metals and the semiconductor 12

Figure 1.9 A schottky on n-type semiconductor [A] before contacting [B] after contacting 13

Figure 2.1 6-inch diameter AlGaN/GaN on Si wafer diced into 1cm × 1cm 16

Figure 2.2 Fume hood for sample preparation and cleaning 17

Figure 2.3 Alignment is carried out with Karl Suss MJB3 photo-mask aligner 19

Figure 2.4 Schematic photolithography processes with positive PR and metallization steps (a) Sample is cleaned (b) Photoresist is coated (c) UV exposure (d) Photoresist is developed (e) Metallization (f) after wash the metallized sample with acetone 21

Figure 2.5 DC magnetron Sputtering system 23

Figure 2.6 Sample on the heating strip 24

Figure 2.7 Rapid Thermal Annealing system 25

Figure 2.8 Before annealing (left) and after annealing (right) 26

Figure 3.1 Keithley 2410 Source meter and a probe station 29

Figure 3.2 Variation of the depletion-layer width and output characteristics of a MESFET under various biasing conditions 31

Figure 3.3 Id-Vd measurement of HEMT by changing applied gate voltage 32

Figure 3.4 Capacitance voltage measurement 33

Figure 3.5 Capacitance voltage measurement system 35

Figure 4.1 ID-VDS characteristics measured at gate voltage of (a) 1 to -4V and (b) to -6V 37

Figure 4.2 Schematic sample structure and configuration of photoionization measurement 38

Figure 4.3 AlGaN/GaN HEMT structure on p-type Si substrate 39

Figure 4.4 Schematic configuration of spectroscopic photo I-V measurement system 40

Figure 4.5 Spectroscopic photo I-V measurement with respect to different wavelengtgh (a) is from the top, (b) is from middle, and (c) is from bottom 42

Figure 4.6 Current vs Wavelength graphs with two different voltages applied on, and Responsivity (current/power intensity of wavelength) vs Wavelength graphs of three different samples with different voltages applied on 45

Figure 5.1 Schottky diode after breakdown 48

Figure 5.2 Dependence of breakdown voltage on total epitaxial layer thickness 50

Figure 5.3 Breakdown measurement of different dimensions Schottky didoes 50

Figure 5.4 Size dependence of breakdown voltage with different sweeping directions 51

List of Abbreviations

HCP	Hexagonal Close Packed
FET	Field Effect Transistor
HEMT	High Electron Mobility Transistor
HFET	Heterostructure Field Effect Transistor
2DEG	Two Dimensional Electron Gas
CVD	Chemical Vapor Deposition
TCE	Trichloroethylene
RPM	Revolution Per Minute
UV	Ultra Violet
PR	Photo Resist
DC	Direct Current
RTA	Rapid Thermal Annealing
IR	Infra Red
MOCVD	Metal Organic Chemical Vapor Deposition

Chapter One

Introduction and background

1.1 Introduction

Gallium nitride (GaN) is a binary III-V direct band gap semiconductor. It has been highly regarded as a promising material in the semiconductor field for high power electronics and optoelectronics due to its materials characteristics. As one of III-V nitrides compounds, GaN, same group materials such as AlN or InN, and their alloys are wide band gap materials crystalizing in three common crystal structures, wurtzite, zincblende, and rock-salt structures.[1] Of these crystalline structures, the most common crystal type for GaN is a wurtzite structure because of its thermodynamically stability.

The wurtzite structure possesses a hexagonal unit cell with two idnependent lattice constants, a and c. It is composed of 6 atoms of each type. The wurtzite structure consists of two interpenetrating Hexagonal Close Packed (HCP) sublattices, each with one type of atom, offsetting along the c-axis by 5/8 of the cell height.[2] The figure 1.1 shown below is the structures of wurtzite and zincblende.

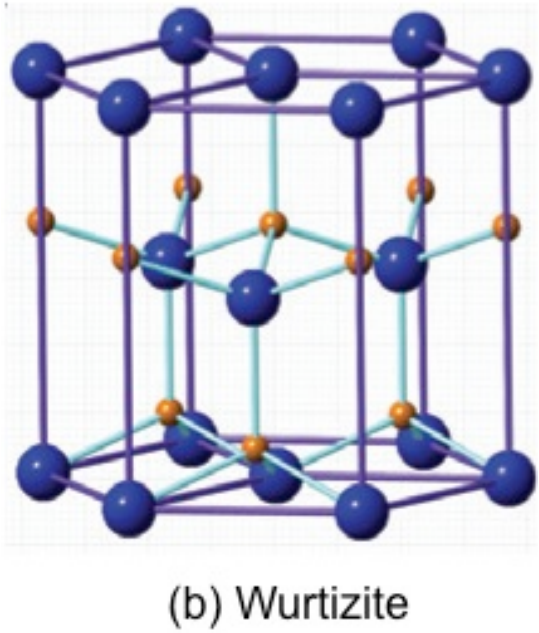

Figure 1.1 Wurtzite structure of GaN[3]

Gallium Nitride (GaN) is a fundamental material of III-V group used for various applications in electronic devices such as high temperature, high power, and high frequency transistors. First attractive property of GaN is thermal stability. GaN as wide-band gap material having band gap energy (3.4 eV) can sustain under much higher temperature than other materials such as Ge, Si, and GaAs. In other words, GaN based power electronic devices will operate properly with inexpensive cooling method which extracts heat out of system. Second, they have high breakdown voltage, which means the device can survive in high voltage/power operating condition. The breakdown field scales approximately with the square of the energy band-gap, and is estimated to be >3.3MV/cm for GaN, as compared to 0.2 and 0.4MV/cm for Si and GaAs, respectively. In addition, Gallium Nitride has excellent electron transport properties, including high electron mobility, and high saturated drift velocity.[4]

Table 1.1 shows breakdown field and related electric properties of GaN and other various semiconductor materials. Based on these properties, Gallium Nitride is typically considered as basic material used for device layers requiring fast carrier transport with a high breakdown voltage and it is used as the channel material in different type of FETs.

Material	Breakdown field (MV/cm)	Band gap Energy (eV)	Dielectric constant (-)
Si	0.3	1.12	11.9
GaAs	0.4	1.43	12.5
InP	0.45	1.34	12.4
GaN (WZ)	3.3	3.43	9.5
AlN (WZ)	8.4	6.2	8.5
InN (WZ)	1.2	0.7	15.3
BN (C)	2-6	6.4	7.1
4H-SiC	3.5	3.2	10
6H-SiC	3.8	2.86	10
Diamond	5	5.6	5.5

Table 1.1 Breakdown fields, band gap energies, and dielectric constants for various semiconductor materials[5]

Due to these superior electronic properties mentioned above, GaN has been attracted to researchers as suitable semiconductor material for power electronic devices. HEMTs (High Electron Mobility Transistors), also known as HFET (Heterostructure Field Effect Transistor), is one type of transistors which has received an attention for use of electronic device applications with benefits of superior properties of GaN and their alloy materials. Of the HEMT devices, AlGaN/GaN based HEMT structure is predominant.[6]

In this thesis, I will focus on AlGaN/GaN HEMT. AlGaN is an alloy of aluminum nitride and gallium nitride that is deposited on top of GaN. By alloying GaN with AlN, a band-gap of GaN can be extended., The band-gap of the alloy varies depending on the Al/Ga ratio and temperature. As the compositional ratio of x in $Al_xGa_{1-x}N$ alloy is changed, the ranges of band-gap energy would be altered.[7] Intrinsic polarization electric field inside AlGaN/GaN heterostructure induces a two-dimensional electron gas that increases proportionally to the composition of Al. Figure 1.2 shows temperature and x composition dependence of ban-gap energy of $Al_xGa_{1-x}N$ alloy.

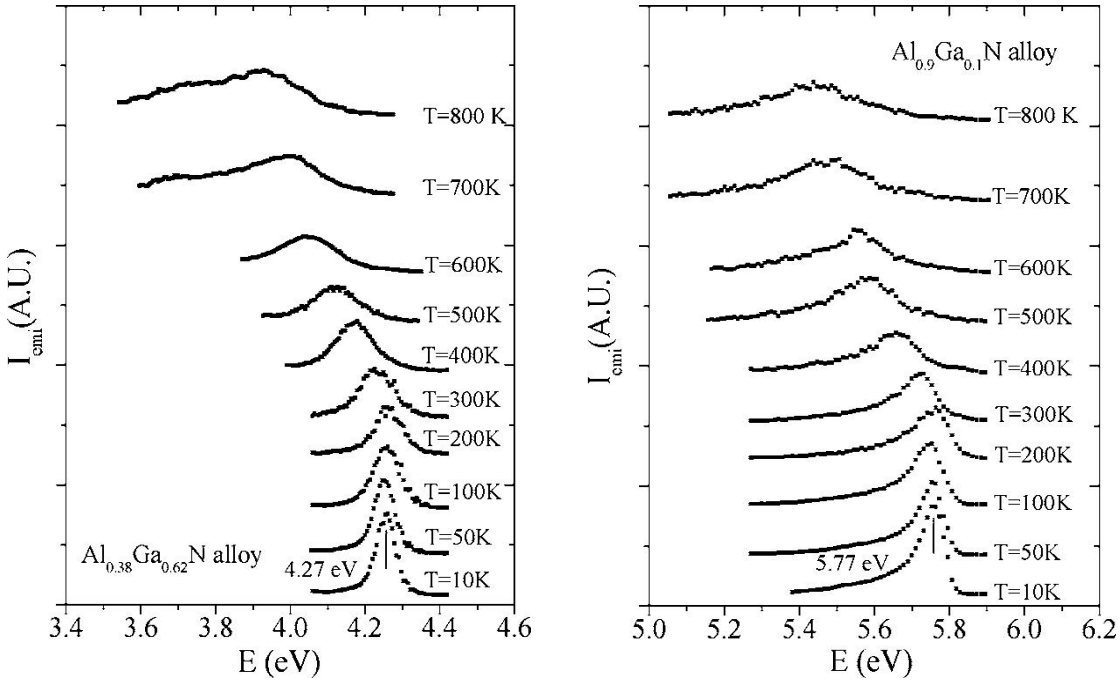

Figure 1.2 PL spectra at different temperature and x composition of Al_xGa_xN[6]

The difference in band structure between AlGaN and GaN layer induces band bending, resulting in triangular quantum well at the interface of two layers. HEMTs have shown excellent

electrical advantages such as high electron mobility and electron concentration due to two dimensional electron gas channel. The high electron mobility is achieved due to their polarization characteristics. The structure of AlGaN/GaN based HEMT is shown in figure 1.3.

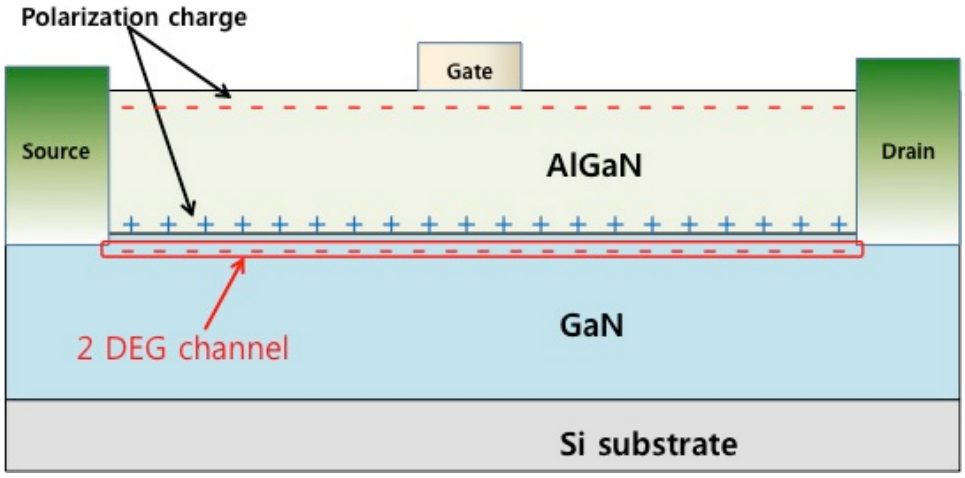

Figure 1.3 AlGaN/GaN based HEMT structure

There are two main factors that affect total polarization. In the AlGaN/GaN HEMT, both spontaneous polarization and piezoelectric polarization influence total magnitude of polarization under tensile strength.[8] It has been studied that piezoelectric polarization is induced by lattice mismatch between GaN and AlGaN owing to their different crystal lattice structure. The difference in lattice structure of AlGaN film on the GaN layer undergoes tensile strain contributing to sheet carrier concentration on the layer surfaces of AlGaN. The band bending is caused as shown below in figure 1.4 due to the transition of Fermi level, and higher electron density confinement in the electron channel of the transistor will be induced due to the piezoelectric polarization and the spontaneous polarization.[9] This piezoelectric polarization in AlGaN layer is about five times larger than that of GaAs based HEMT device. In addition to piezoelectric polarization, many of studies related to HEMT devices have shown that nitride

semiconductors contain spontaneous polarization occurring at interface of AlGaN and GaN layers under zero strain. Spontaneous polarization is a polarization within materials without additional electric field applied, and the total polarization can be defined as summation of spontaneous polarization and strain-induced or piezoelectric effect.[10]

Lately, researchers have indicated that local strain fields related to threading dislocations is able to induce significant electrostatic sheet charge concentrations. Polarization charges in nitride semiconductor structure tend to contribute to decrease of leakage current without increasing aluminum composition in the $Al_xGa_{1-x}N$ layer.[11]

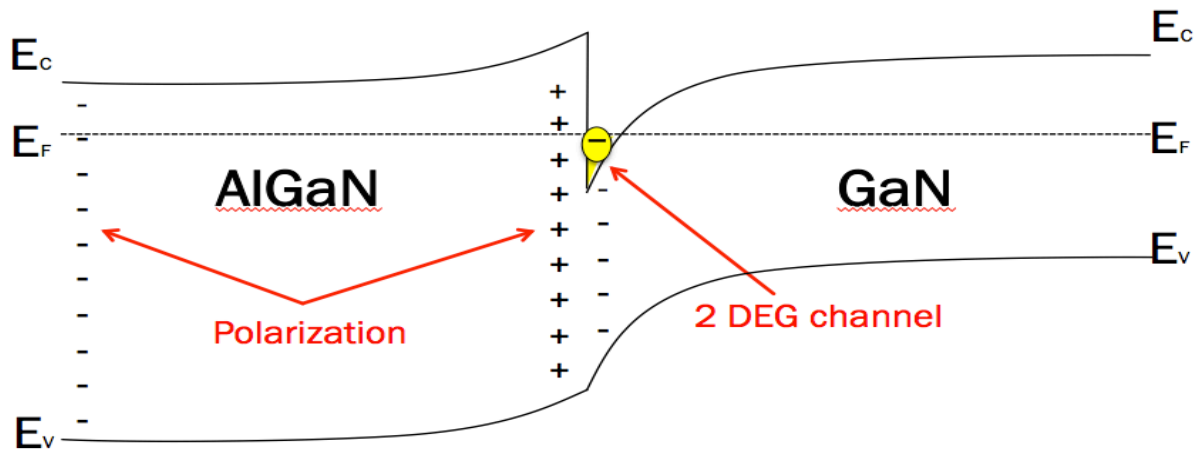

Figure 1.4 Band structure of AlGaN/GaN based HEMT

HEMTs was started fabricating with a GaAs material first because GaAs has higher electron drift mobility in two dimensional electron gas, however, the other electric features such as electron and saturation velocity, thermal stability in harsh environment and sustainability at higher voltage are more adequate for high power devices, with those better features GaN has been considered as more proper material for high power applications.

The existence of 2DEG (Two-Dimensional Electron Gas) at the interface between AlGaN and GaN layers is the dominant reason why AlGaN/GaN based HEMT has more excellent electron transport property than other conventional HEMT such as GaAs.[6] The major difference between AlGaAs/GaAs and AlGaN/GaN is that unlike the AlGaAs/GaAs heterostructure, AlGaN/GaN is able to induce quite large spontaneous polarization and piezoelectric polarization effect without any intended doping, which leads to two-dimensional electron gas channel that has higher electron mobility due to less collisions between ions and electrons.[9] If both of spontaneous polarization and the piezoelectric polarization are induced enough, charge sheet in AlGaN layer will be formed by different spontaneous polarization coefficients and lattice mismatch between GaN and AlGaN respectively. The conduction band of GaN will be bent, forming a triangular quantum-well in which electrons can be trapped. The quantum well at the interface of AlGaN/GaN layers will form two-dimensional electron gas (2DEG)channel. The figure 1.5 below shows how the polarization induces the 2DEG.

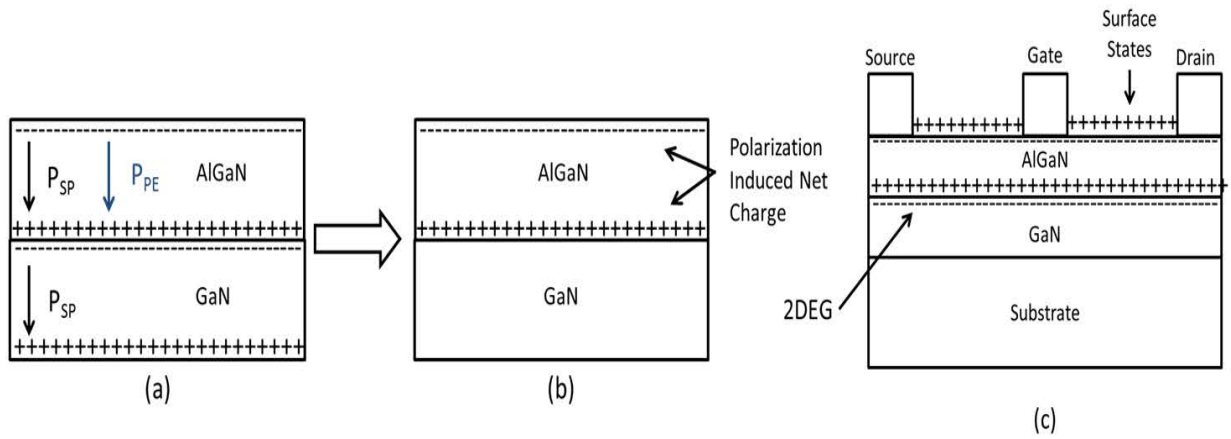

Figure 1.5 (**a**) Individual polarization charge contributions (**b**) Polarization induced net charge (**c**) the AlGaN/GaN HEMT with polarization induced net charge and surface charge contributions[6]

Those confined electrons in 2DEG channel exhibit higher electron mobility than AlGaAs/GaAs HEMT since AlGaN/GaN heterostructure generates two dimensional electron gas without

deliberate additional doping, which means the electrons in the channel are subject to less electron scattering due to smaller number of impurities in the channel. In order to understand the 2DEG, it would be the starting point to interpret the two dimensional electron gas channel mobility.[12] The electron mobility in the 2DEG is principal determinant of electrical performance of HEMT devices. Various scattering mechanisms such as ionized impurity scattering, polar optical scattering, acoustic phonon scattering, and piezoelectric scattering affect the total mobility in 2DEG channel depending on their specific temperature.[4] Figure 1.6 indicates the temperature dependence of electron mobility in bulk GaN.

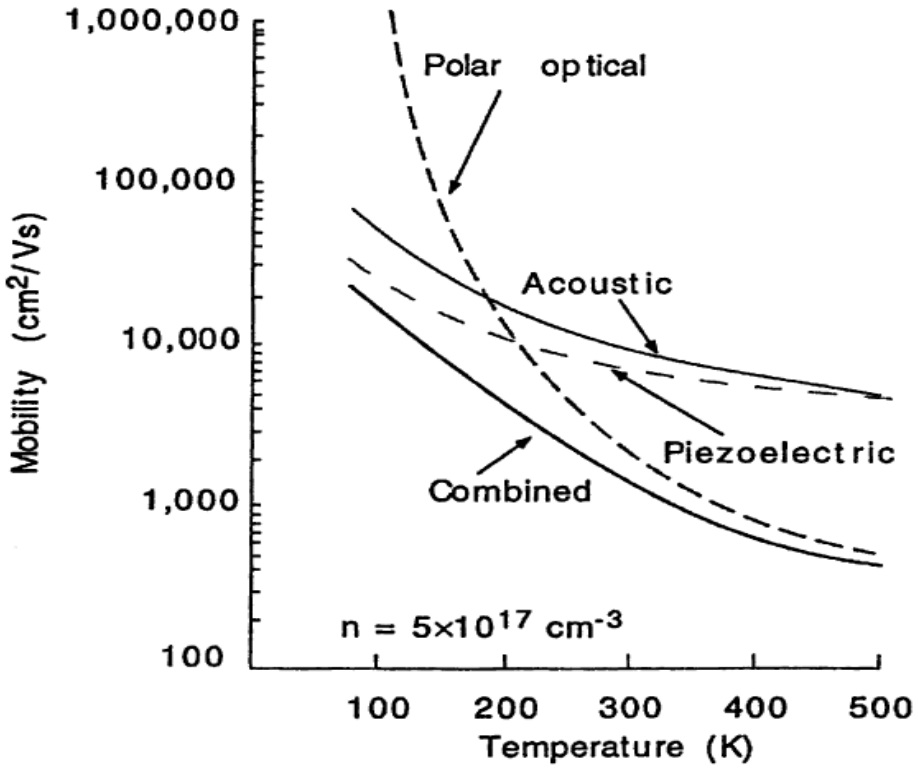

Figure 1.6 Contributions to electron mobility of different mechanisms in GaN[4]

One of the superior properties of AlGaN/GaN based HEMTs is high carrier density. The carrier concentration, however, can be influenced by the existence of impurities or defect inside of the

heterostructure.[13] It has emerged that defects or impurities in lattice structure or interface of the multilayers in heterostructure are associated with electron trapping within devices, inducing a current collapse which degrades the attainable device performance. Current collapse usually is a result from electron carriers trapped at defects or impurities in the device. The trapping phenomenon of electron carriers in 2DEG channel is a particular concern. As drain-source voltage is applied to the device, charge carriers can possibly be trapped at specific sites where the device includes a high concentration of trap.[14] The trapped carriers still stay even after drain-source voltage applied is removed resulting in degradation of output power of the device. The current collapse on output power can be observed through current-voltage characteristic of FET in figure 1.7.[15]

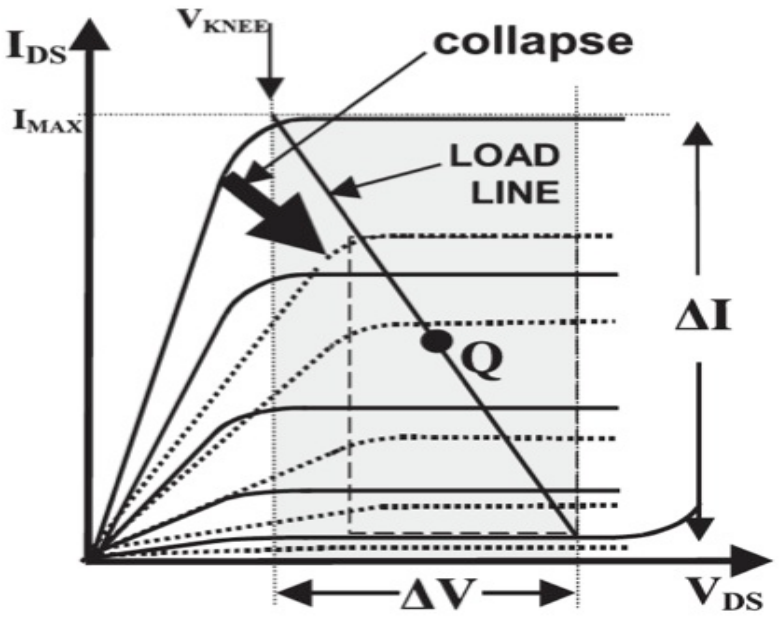

Figure 1.7 A sketch of FET I–V characteristics before (full curves) and after (dotted curves) current collapse. The maximum attainable device output power is approximately proportional to the area of the shaded and broken rectangles, before and after collapse, respectively[15]

In order to gain higher output power from the device, current collapse induced by trapping should be suppressed. Photoionization has been used as an experimental method that can be

applied to reduce the current collapse by illuminating light. A light illumination on the device enables the trapped carriers to have enough energy to be released from the traps. Once the carriers trapped at defects absorb sufficient energy to overcome the threshold, trapped carriers start to be released, restoring collapsed current. Consequently, with the aid of photoionization technique, the reduced output power owing to current collapse caused by carrier traps can be recovered. By using the phenomena of restoration of current collapse, photoionization spectroscopy has been employed to probe identification of the traps that definitely cause current collapse. As illuminated light on the device increases to excite trapped carriers, the drain current as well increases since de-trapped carriers drift back to 2DEG conducting channel. During this process, measured spectrum can show unique property of each defects since each traps, defects or impurities have their own unique threshold energy, lattice coupling, and absorption cross section, all of which can be used to identify the nature of the defects.[15] Therefore, photoionization technique may be employed to analyze the defects within the structure.

With the overall properties such as high electron mobility or 2DEG formation we discussed so far, GaN based HEMTs is suitable for high power applications providing outstanding electrical properties compared to traditional semiconductor materials. It has been scrutinized that GaN device has higher output power, operational voltage, and operating temperature than other conventional GaAs or SiC based transistors, which leads GaN to more suitable to radio-frequency power amplifiers. Furthermore, its thermal stability, high current density due to the presence of 2DEG, and high breakdown voltage also enable GaN to be more attractive material satisfying more advanced technology for electric applications in the future.

Background

1.2 Ohmic contact

Depending on what metal is used as a contact to a semiconducting material, different electrical characteristics are expected. Metal contacts on semiconductor can be ohmic contacts which have a linear current-voltage characteristics following the Ohm's law and non-ohmic contact such as schottky barrier, p-n junction, or rectifying heterojunction that do not show an ohmic behavior. Typically, ohmic contact can be formed as metal-metal or metal-semiconductor ohmic contacts. In this thesis, metal-semiconductor ohmic contact will be a focus. In order to form an ohmic contact to a semiconductor, it is carefully required that ohmic contact should have low resistivity to show ideal ohmic contact property. The primary requirement to be an ideal ohmic contact is low-resistance since ohmic contact has to allow electric current to flow in both directions between metal and semiconductor. Having as low resistance as possible of ohmic contact determines the performance of semiconductor. In other words, poorly fabricated ohmic contact on semiconductor frequently displays rectifying behavior leading ohmic contact to have a depletion region that may block electric current between metal and semiconductor. Metal-semiconductor ohmic construction can be commenced from stacking metal layers up, using various deposition systems such as sputtering deposition and chemical vapor deposition (CVD). In this thesis, the multilayers of Ti/Al/Ti/Au has been chosen as ohmic metal layers on AlGaN/GaN HEMT device. Designed ohmic contact model of AlGaN/GaN HEMT is in figure 1.8.

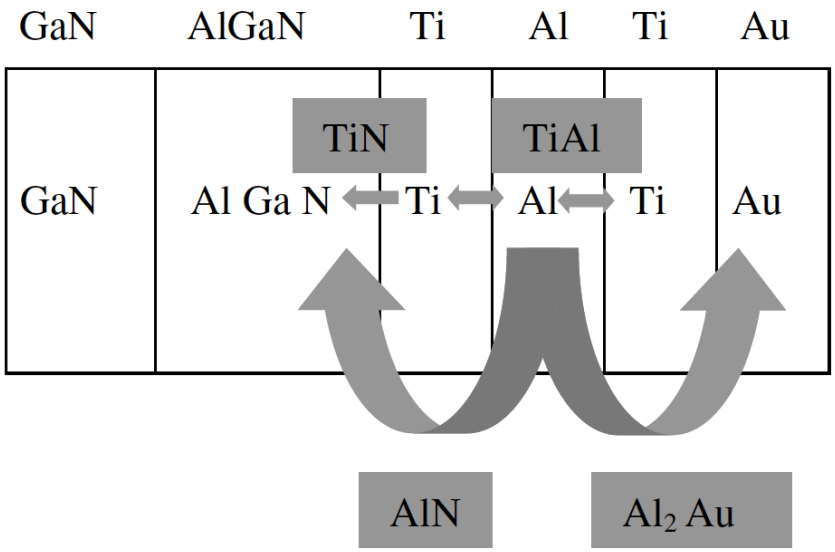

Figure 1.8 Reactions among different metals and the semiconductor[16]

The formation of ohmic contact in general is to anneal the metal contact on the semiconductor so that the ohmic metal which is Ti/Al binary layer can diffuse into semiconductor. High temperature heating in short amount of time leads ohmic metal to be blended with semiconductor components lowering the barrier between the metal and semiconductor. The ohmic contact mixed with semiconductor material also produces N vacancies by extracting Ti out of GaN based on thermal annealing.[17] High concentration of N vacancies acts as donors near the interface, inducing band banding.[18] Therefore, heavily doped area causes easier tunneling due to the narrowed barrier width.[19] It has been indicated that Ti/Al binary layer is highly important to formation of low resistance ohmic contact, allowing electron charges to flow in both directions. Ti/Au binary layer on top of the Ti/Al layer is a purpose of preventing Ti/Al binary layer from oxidization and Au diffusing into the Ti/Al layer.

1.3 Schottky contact

As one of non-ohmic metal junction, schottky contact is representative. A schottky diode which is also metal-semiconductor junction has higher schottky barrier than ohmic contacts so that they can rectify current flow between metal and semiconductor. In the case of n-type semiconductor such as n-type GaN and metal junction, schottky contacts can be formed when the work function of metal is higher than the electron affinity of n-type semiconductor due to formation of the barrier between metal and semiconductor.

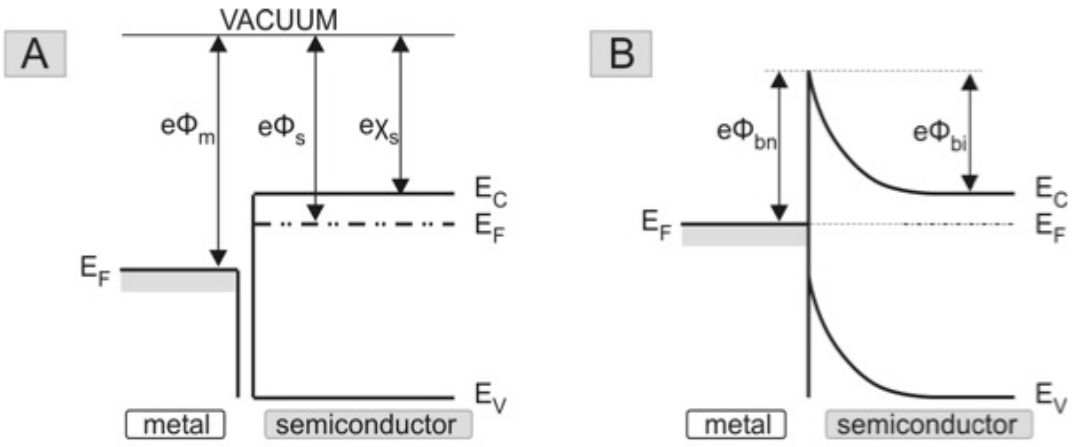

Figure 1.9 A schottky on n-type semiconductor [A] before contacting [B] after contacting[20]

The formation of schottky barrier is shown in the figure 1.9, where Φ_m is work function of metal, Φ_s is work function of semiconductor, and χ_s is electron affinity of semiconductor. When both metal and semiconductor are in contact, each of Fermi levels has to be in constant lowering conduction band and Fermi energy level of semiconductor. The height of barrier, which is known as schottky barrier, Φ_{bn} is given by

$$\Phi_{bn} = (\Phi_m - \chi_s)$$

When the barrier height, Φ_{bn}, is high enough schottky barrier operates as rectifier due to depletion region at interface of metal-semiconductor junction. Small bias applied to schottky contact cannot overcome the barrier. However, under large bias, the electron carriers can jump up, inducing current passing through the barrier. Upon forward bias, electrons within the semiconductor are excited which allows them to go over the barrier, resulting in current flow in the opposite direction. In contrast, under reverse bias, as the electrons obtain enough thermal energy to surpass the barrier height, leakage current is generated.

It is essential for power device to possess schottky contact with ideal electrical properties such as high breakdown voltage, and low gate leakage current. The leakage current is the dominant drawback for AlGaN/GaN HEMT device, hence the understanding of leakage current flow in schottky diode is required.[21] The dominant mechanism for high leakage current is due to high probability of defect-assisted tunneling effect and other conduction mechanisms induced by poor quality of inhomogeneous interface and highly conductive dislocations within metal-semiconductor interface.[22]

The governing carrier transportation mechanism for leakage current in case of reverse bias applied is the emission of electrons out of trapped state neighboring the interface of metal-semiconductor into continuum of states related to conductive dislocations.[23] Ni and Au, as schottky contact materials, are suitable material in order to reduce leakage current due to high work function of Ni (5.15eV) and Au (5.1eV) inducing high schottky barrier height $\Phi_{bn.}$[24] Moreover, it has been noticed that Ni and Au are widely used metal because of its excellent adhesion to nitride and high thermal stability, respectively.[25]

Chapter Two

Device Fabrication

2.1 Introduction

In this chapter, HEMT fabrication steps, technique, and semiconductor processing system will be described with theoretical details and experimental procedures. The fabrication steps consist of cleaning, photo-lithography, metal deposition, and annealing. After fabrication, typical semiconductor measurement techniques such as current-voltage measurement and capacitance-voltage measurement are used to analyze the device characteristics. Data resulted from HEMT device measurements will be presented below.

2.2 AlGaN/GaN wafer preparation

In this experiment, 6 inch diameter HEMT wafer diced into 1cm×1cm was used for device fabrication. The AlGaN/GaN HEMT layer was grown on silicon substrate and the layer structure is composed of AlN layer (0.25μm), AlGaN (0.5μm, 55-75% of Al), AlGaN (0.5μm 40-50% of Al), AlGaN (0.7μm, 20-25% Al), GaN (1μm), AlGaN (10-20nm, 25% of Al), GaN (2nm). Figure 2.1 shows typical AlGaN/GaN HEMT wafer we used for device fabrication.

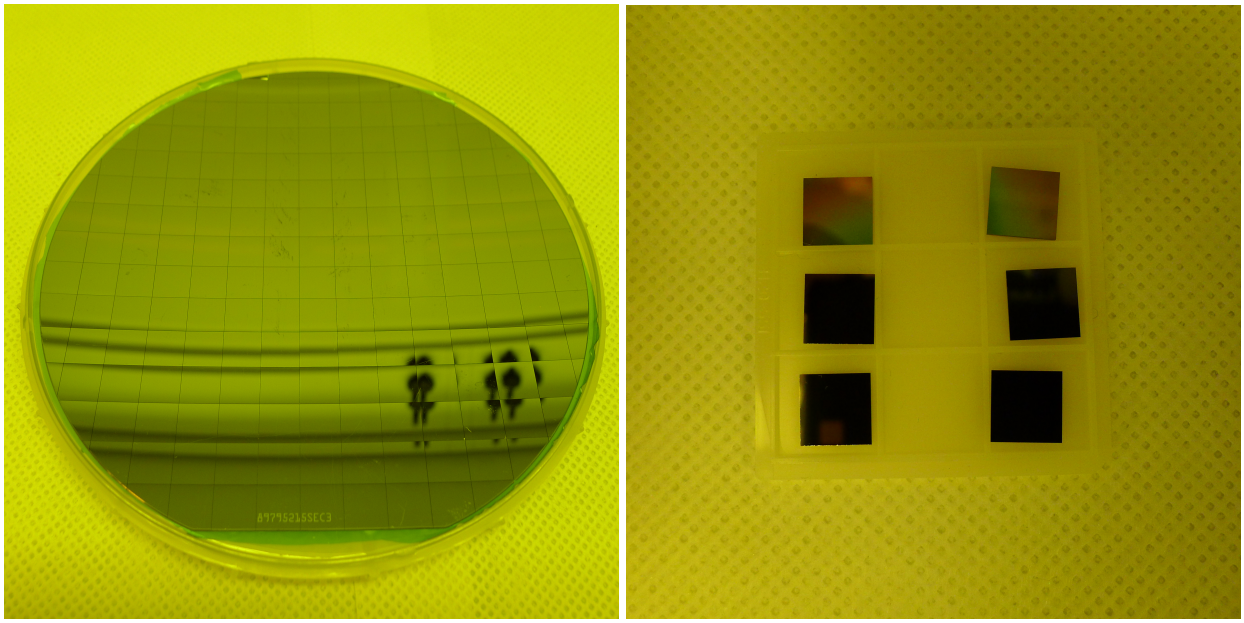

Figure 2.1 6-inch diameter AlGaN/GaN on Si wafer diced into 1cm × 1cm

2.3 Cleaning

As the first step of device fabrication procedures, it is not an exaggeration to mention that cleaning step is the most important part for great quality of device property. The main objective of cleaning step is to remove organic, oxide, and ionic contaminants on the wafer. The GaN cleaning steps are performed under fume hood with ventilation system. In order to remove organic contaminant on the wafer, different chemicals are utilized. Each of cleaning process takes 5 minutes in the ultrasonic cleaner in the following order: acetone, trichloroethylene (TCE), acetone, methanol, and methanol again. First, the diced wafer is immersed into acetone to degrease organic contaminants on the surface of sample then dip into trichloroethylene (TCE) for further cleaning. Second, acetone solvent immersion serves as TCE residue removal from the sample. Then, first methanol is used in order to dissolve acetone residue, then second immersion into methanol is required for further cleaning.

The last step of removal organic contaminant is to rinse the sample with deionized (DI) water to remove solvent residue. After removal of organic contaminant, additional steps for ionic contaminant and native oxide are required. Submersion into 1:1 ratio mixture of DI water and hydrochloric acid (HCL) for 10 minutes at temperature 110°C removes ionic contaminant and native oxide on surface of sample. It has been studied that the hydrochloric acid cleaning is efficient to diminish oxygen concentration on the surface.[26] In addition to reduction of oxidization, Cl residue after HCl treatment can enhance adhesion of metal to the surface of semiconductor.[6] Final step is washing the sample with DI water and dry with nitrogen air gun.

Figure 2.2 Fume hood for sample preparation and cleaning

2.4 Photo-Lithography

A principal step of the HEMT fabrication process is to transfer the pattern on the photo mask to the substrate. In order to accomplish this, photolithography is the key technique. Photolithography is an optical process by using light source from the exposure system. Photolithography procedure has several steps: photo resist (PR) application, baking, mask alignment, exposure and development. After finishing cleaning steps, diced sample needs to be attached to the substrate first, in this case we used 3-inch dummy silicon wafer as a substrate and used photoresist to stick the sample to the substrate. After drying the attached sample about for 30 to 60 seconds, the sample is located it in the furnace for 1 minute to dry it out. This process will improve adhesion so that it is not detached from the substrate during the spin coating process. Then, the sample is coated with reversible photoresist, AZ5214-E, by using spin coater in mode D with 4,000 RPM to cover the sample with uniform thickness. Across the sample, the thickness is dependent on many different factors such as spin coating speed, substrate, humidity, and viscosity of the PR. The thickness of the photoresist on the sample can be described as follows.

$$Thickness = k\frac{p^2}{\omega^{1/2}}$$

where k is constant of the spinner, p is the resist solid content, and w is a revolution per minute (RPM) of the spinning. The average thickness of the photoresist coated with 4,000 RPM is 1.5 micrometer. Once it is coated completely with photoresist, the sample is pre-baked for 1 minute at 110 ℃ so that the photoresist can be more sensitive to the light source by evaporating the solvent out of photoresist. Next step is mask alignment. The sample covered with photoresist is aligned with mask and is exposed to the UV radiation produced by Hg arc lamp at the power of 160 watt for 30 seconds.

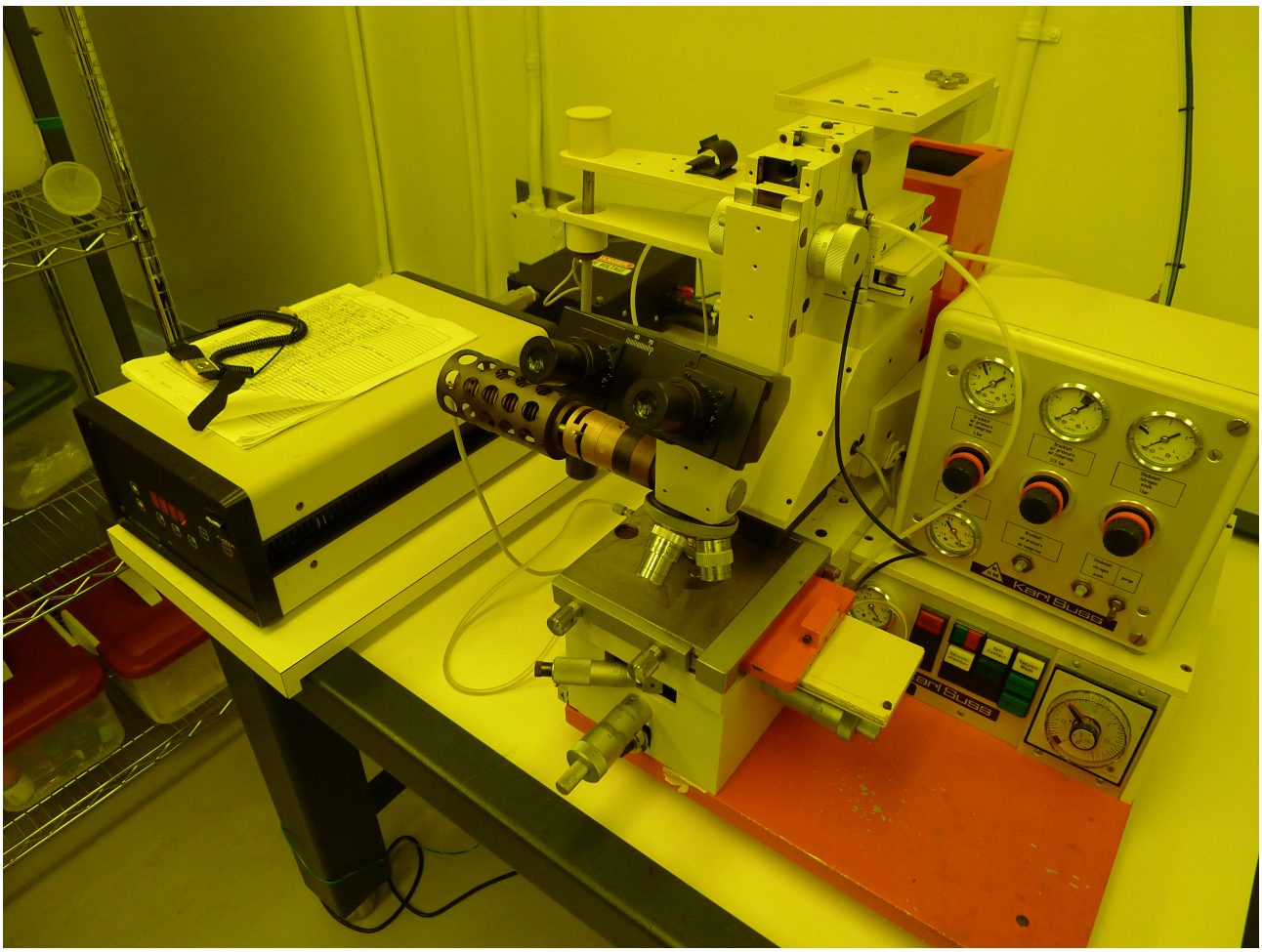

Figure 2.3 Alignment is carried out with Karl Suss MJB3 photo-mask aligner

The exposed photoresist experiences different chemical reaction depending on the type of PR (positive or negative PR). In the case of negative PR, the region exposed to UV light becomes polymerized and will be hardened to be removed by an etchant. After exposure of sample, post baking should be carried out for reversal image. The sample post-baked for 60 seconds at 110 ℃ has both insoluble area and photoactive area where were originally exposed area and unexposed area, respectively. Then, the sample is exposed again for 60 seconds at 110 ℃, which is called flood exposure. This repeated steps are the most critical procedure of reverse photolithography.

As a result, there will be only photoresist remained on the sample where UV light was unexposed on originally through reversal image process. On the other hand, in positive photolithography process photoresist will remain only where the UV light was exposed on the sample. As the last step of the photolithography, the prepared sample will be immersed into developer which is the mixture of water and developer solution with the ratio of 1:1 to get the mask pattern image.

The overall photolithography procedure requires several steps below;

1. Sample preparation
2. Coating the sample with the PR (depending on type of PR, negative photoresist or positive photoresist can be adopted)
3. Pre baking for better sensitivity and adhesion
4. Exposure to UV light
5. Post baking and flood exposure (if needed to make reversal image)
6. Development

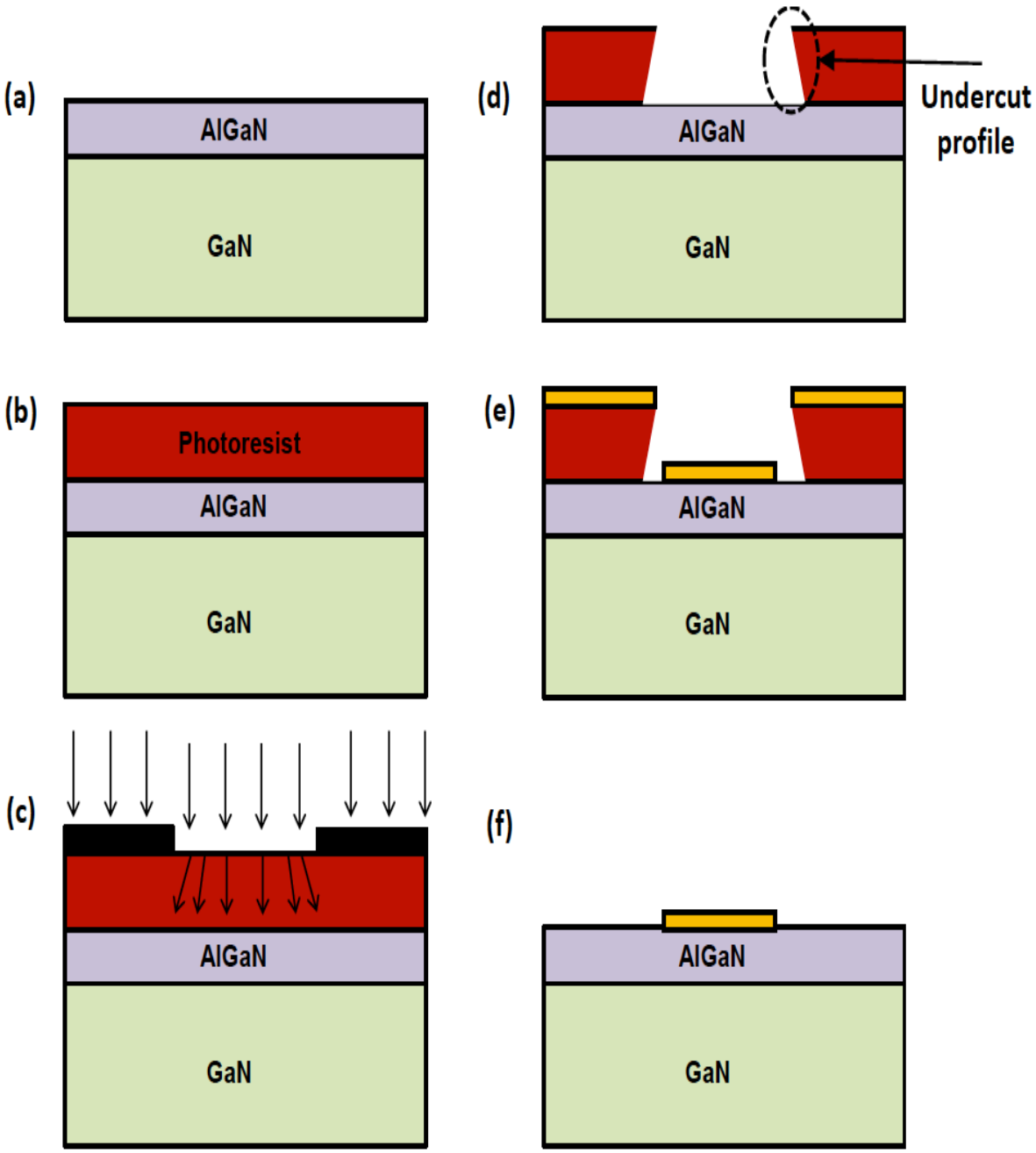

Figure 2.4 Schematic photolithography processes with *positive PR* and metallization steps (a) Sample is cleaned (b) Photoresist is coated (c) UV exposure (d) Photoresist is developed (e) Metalization (f) after lift off the metallized sample with acetone[27]

2.5 Metallization

As one of physical vapor deposition method, DC magnetron sputter is used to deposit thin film onto AlGaN/GaN substrate. Before sputtering, the chamber of the sputtering system will be fully filled with the inert gas such as Argon (Ar). Then, Argon is accelerated by high voltage applied on them. Positively charged argon gas will be attracted toward target which is negatively charged by system. The impinging argon atoms and the target will experience ion bombardments. If the momentum of the accelerated atoms is larger than the binding energy of the surface of target, the target atoms can be excited from the target. Then, the ejected target atoms will be deposited on the surface of the AlGaN/GaN sample with help of guidance of equipped chimney on the target. The chimney equipped on the target will help preventing cross contamination over samples as well. At the very beginning process of sputtering, the chamber has to be highly evacuated so that chamber does not have any contaminants inside. By using turbo molecular and mechanical pump, the chamber is pumped down up to 10^{-7} Torr. Once the pressure reach the level of 10^{-7} to 10^{-8} Torr argon gas will be introduced to the chamber for 5 minutes. After achieving 20 miliTorr of pressure with introducing Ar, direct current will be applied to target for generation of plasma. The magnet under the target holders increases the sputter rate by confining the plasma in the case of magnetron sputtering. Pre-sputtering will be conducted for 2 minutes to warm the target up and to remove any contaminants on the target. Deposition rate or sputtering rate that determines the thickness of the deposited metal depends on the target due to different binding energy target material. After the sample is placed on the circular plate which rotates by adjusting the knob, thin metal film will be deposited on sample. Metallization process will be finished after deposition by immersing the sample into the acetone.

Photoresist on the sample will be washed off by the acetone, then there is only metal pattern on the sample. This step is called lift off.

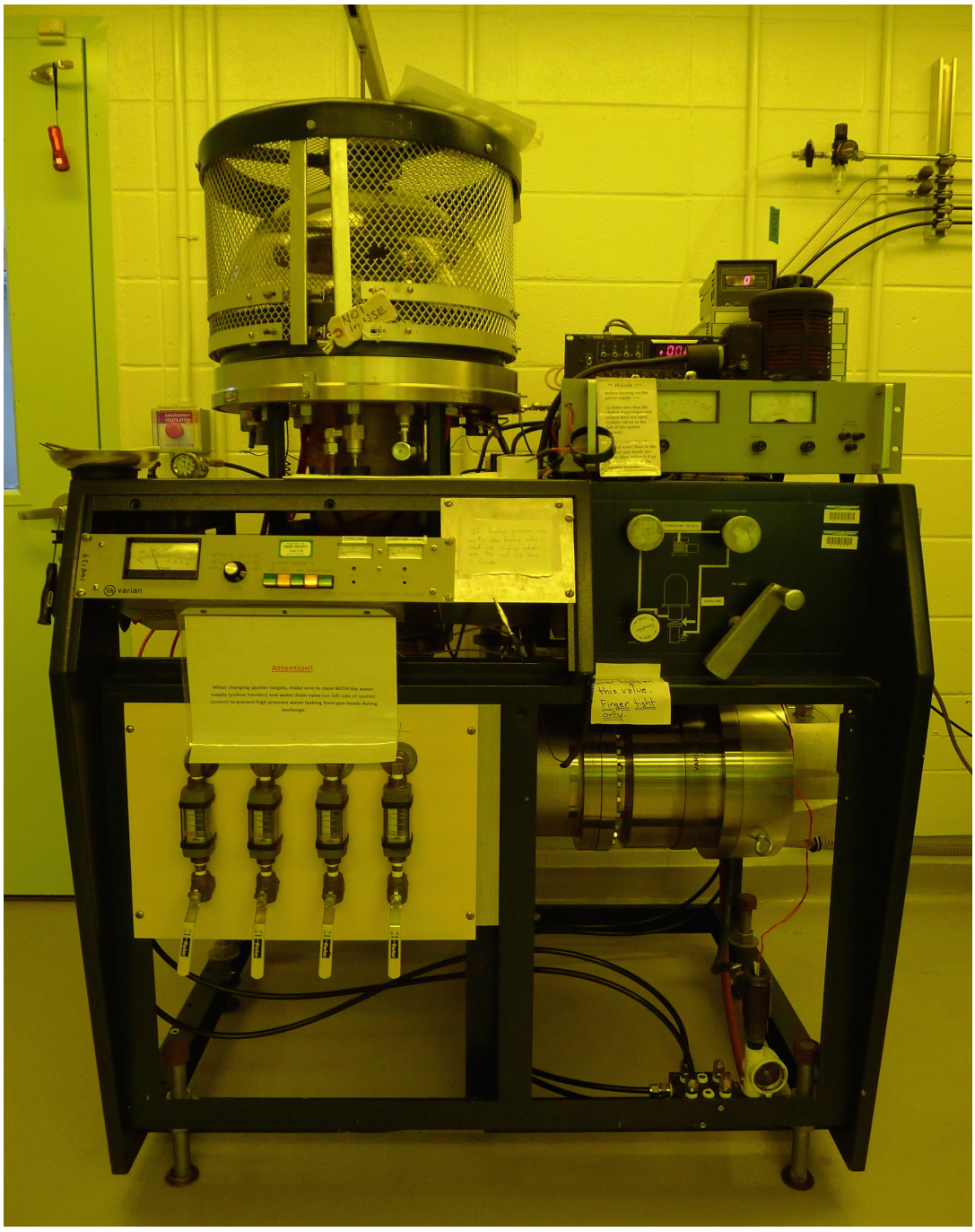

Figure 2.5 DC magnetron Sputtering system

2.6 Rapid Thermal Annealing (RTA)

As an additional step to form an ohmic contact on the surface of semiconductor, rapid thermal annealing system (RTA) is used. By annealing the metal-semiconductor contact at high temperature for a short period of time, the elements in the metal and semiconductor layers will inter-diffuse, forming an alloy. In the case of mulilayered metallic contacts, the interdiffusion will occur amongst the elements that constitutes the metallic layer. Then, the electrical properties of metal/semiconductor will be altered. In the case of the AlGaN/GaN HEMT fabrication, rapid thermal annealing is one of the key processes to form good ohmic contact. The RTA system consists of vacuum chamber, carbon heating strip, and IR pyrometer. The sample is loaded on heating strip inside vacuum chamber. Since it is a lateral device (*i.e,* ohmic and schottky contacts are on the same side), metal deposition is not supposed to be in contact with heating strip to prevent contamination from the strip. The infrared pyrometer is equipped near sample to observe the change of temperature of strip. After loading, the vacuum system will pump out pressure up to 10^{-7} Torr to get rid of contaminants as sputtering system does. Then Nitrogen gas will be introduced to vacuum chamber for 5 minutes up to they chamber is fully filled with N_2 gas. Afterward, temperature will be rapidly elevated up to 850 ℃ by increasing the current through heating carbon strip and heat the sample up for 30 seconds. N_2 gas will be introduced again to cool the system down for 10 minutes to have the room temperature inside vacuum chamber.

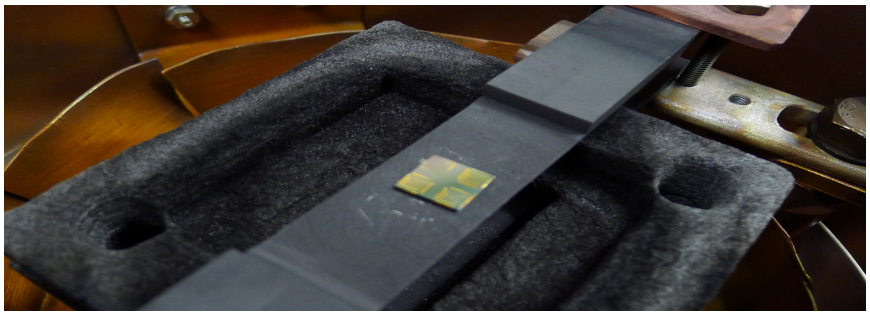

Figure 2.6 Sample on the heating strip

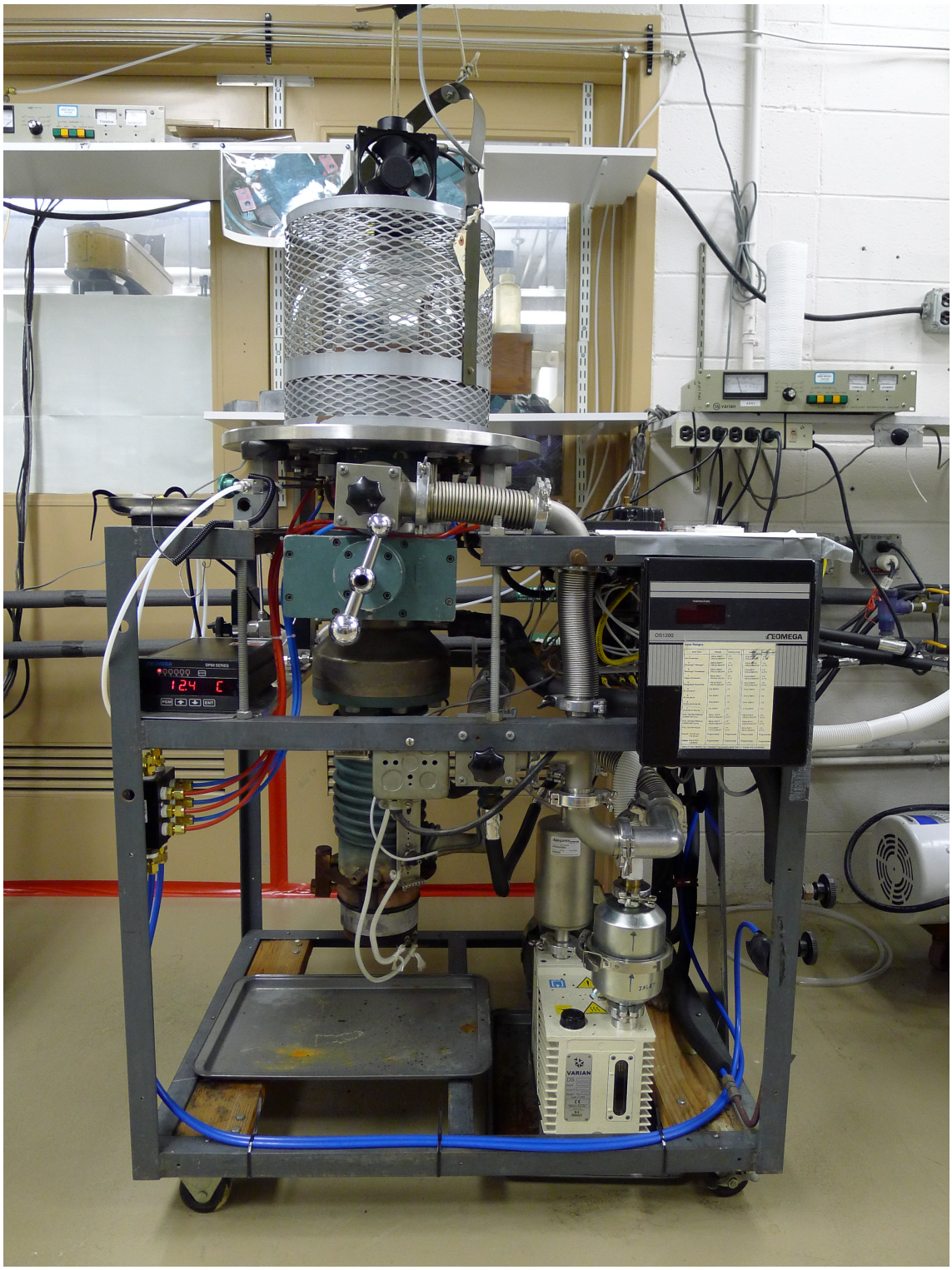

Figure 2.7 Rapid Thermal Annealing system

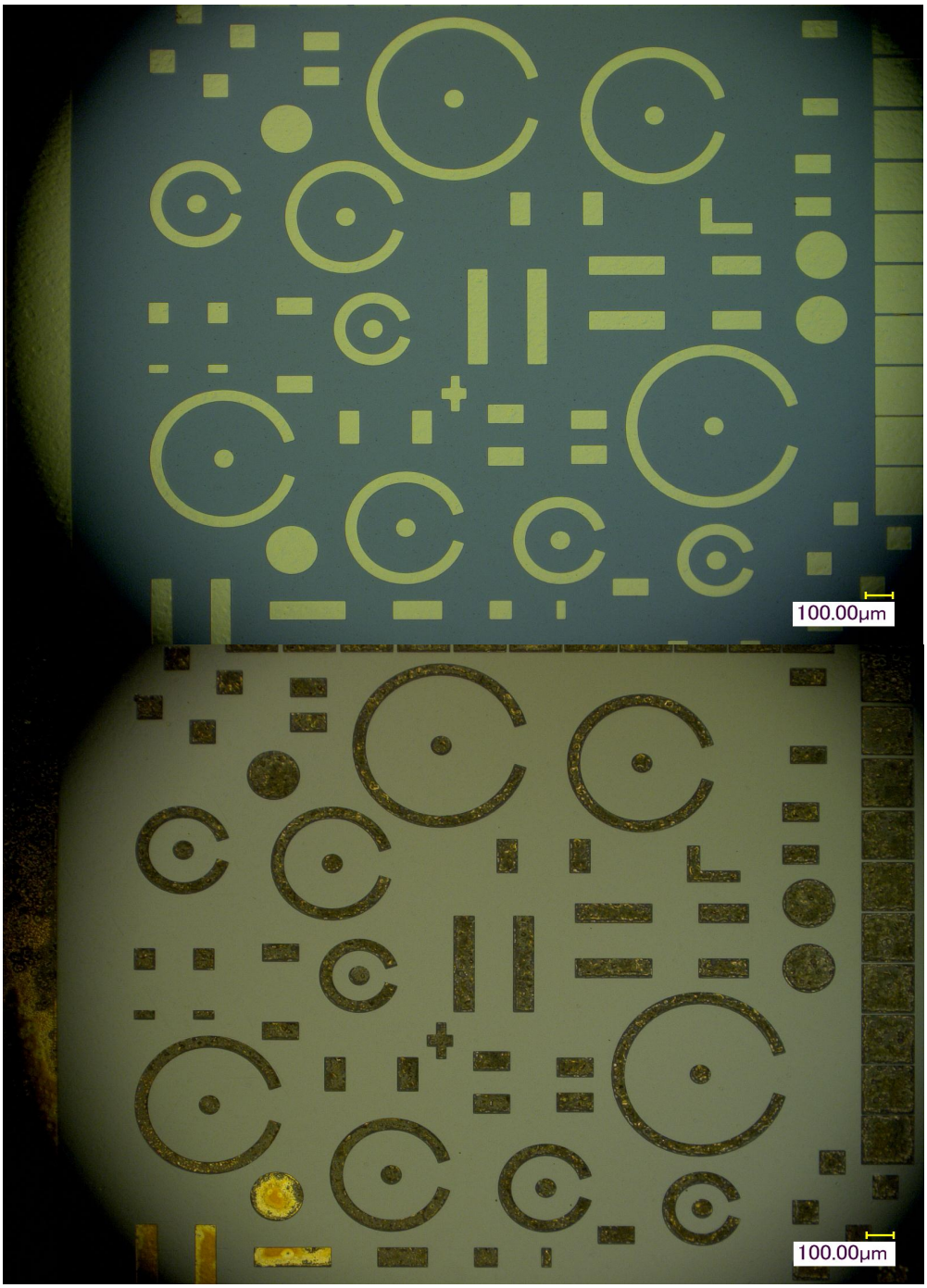

Figure 2.8 Before annealing (left) and after annealing (right)

As shown in the figure 2.8 above, after annealing the metal contact on the sample is diffused into substrate showing changed color and texture. The ohmic contact metal used in this fabrication is Titanium, Aluminum, and Gold with their material properties mentioned below.

1. Titanium - good adhesion to the material and mechanical stability. After annealed, it removes native oxides remained at surface which might extract nitrogen (N_2) from the GaN forming TiN leaving a high density of N vacancies (donors) around the interface, which holds the Fermi level. Electrons then have possibility to tunnel from the 2DEG to the contact with ease.[27]

2. Alumium - Reacts with Titanium forming Al_3Ti preventing oxidation of the Titanium layer. It is also responsible for improving the contact resistance.[27]

3. Gold - Not only prevents oxidation of the contact, also improves conductivity of the contact during operation.[27]

2.7 Summary

Device fabrication has been carried out in order to construct HEMT device. A fabrication procedure requires proper cleaning steps to get rid of all the contaminants on a surface of wafer since organic contaminants or naïve oxygen remained on the wafer will degrade a quality of ohmic contact. A circular shape of HEMT device has an advantage compared to rectangular shaped device. It does not require special isolation of the device such as MESA etching, so circular HEMT reduces fabrication procedure and possible defect during the processing.

Chapter three

Device characterization

3.1 Introduction

As a one of crucial aspect of the semiconductor manufacture field, measurement techniques have been required to be more precise and refined to characterize electrical properties of devices. There are various optical and electrical device measurement methods such as optical microscope, photo conductance, resistivity characterization, I-V measurement, C-V measurement, and transconductance measurement. In this chapter we will mainly discuss about the electrical measurement techniques mentioned above for the AlGaN/GaN based HEMT (High Electron Mobility Transistor) devices.

3.2 Current-Voltage measurement

As one of the conventional electrical measurement techniques, current-voltage measurement has been conducted to characterize and analyze semiconductor devices. It can be easily understood by extracted information from the IV curve of the HEMT device whether the device operates properly as a semiconductor, and also the electrical properties such as pinch off voltage, or saturation current. Current-Voltage measurement has been performed with the help of Keithely 2410 sourcemeter and the probe station as shown in the figure 3.1 below.

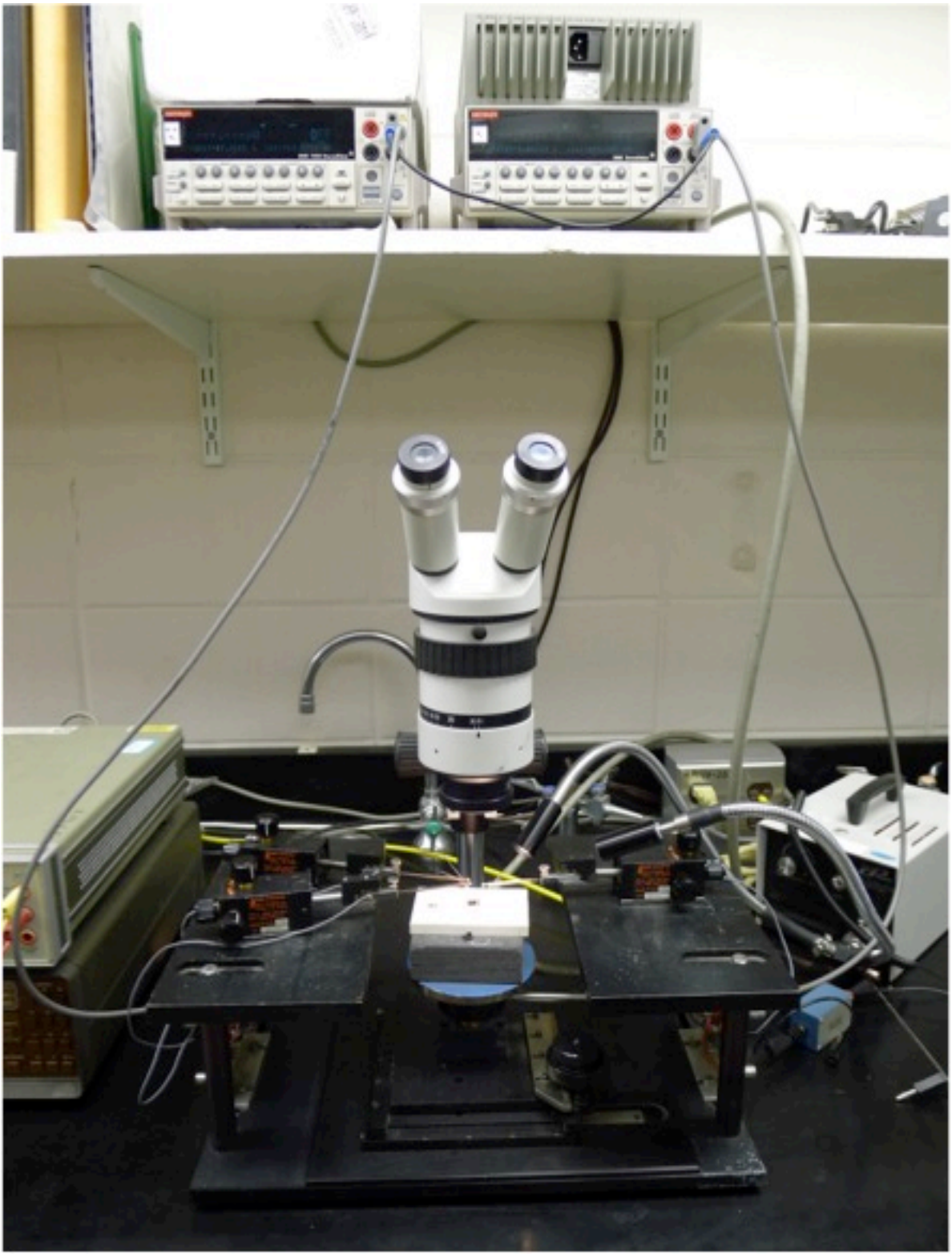

Figure 3.1 Keithley 2410 Sourcemeter and a probe station

The operation principle is quite straightforward. When there is 0 gate voltage applied on the device with very small Drain voltage applied, small Drain current will flow in the channel through two dimensional electron gas channel. The drain current is given by applied drain voltage/resistance (V_d/R) where R is the resistance in the channel. Hence, the drain current through the channel changes linearly with the increase of drain voltage. As the drain voltage increases, depletion region W is increased as well then the cross section area for current flow will be narrower. Therefore, the resistance inside the electron channel will be increased. As a result, the current through the channel increases with decreasing slope as the drain voltage increases. If the drain voltage continuously increases the depletion region will reach to the lower substrate, chocking the electron channel off as shown in the figure 3.2(b) when the width of depletion region is equal to the thickness of the epitaxial layer (W = a) shown in the figure 3.2 (b) is so called saturation drain voltage, $V_{Dsat.}$

$$V_{Dsat} = \frac{qN_D a^2}{2\varepsilon_s} - V_{bi} \quad \text{for } V_G = 0$$

Where, $\frac{qN_D a^2}{2\varepsilon_s}$, is pinch off voltage. By increasing drain voltage, the drain current will eventually saturated since the source and the drain are totally separated by the depletion region. At the location P, which is called pinched-off point, large drain current will pass through the depletion area. As the V_D increases further over the saturation drain voltage the pinched off point will re-locate toward source as illustrated in the figure 3.2(c). Even though the applied drain voltage increases, the voltage at location P as indicated in the figure 3.2(c) remains equal. Therefore, total number of electron carriers reaching from the source to pinched-off point P and corresponding electric current through the channel will remain the same since the change of the potential drop inside the channel from source to pinched-off point P will not change. Hence, if

the applied drain voltage is larger than saturation drain voltage, the drain current will stay on saturation current I_D with nothing to do with V_D.[28]

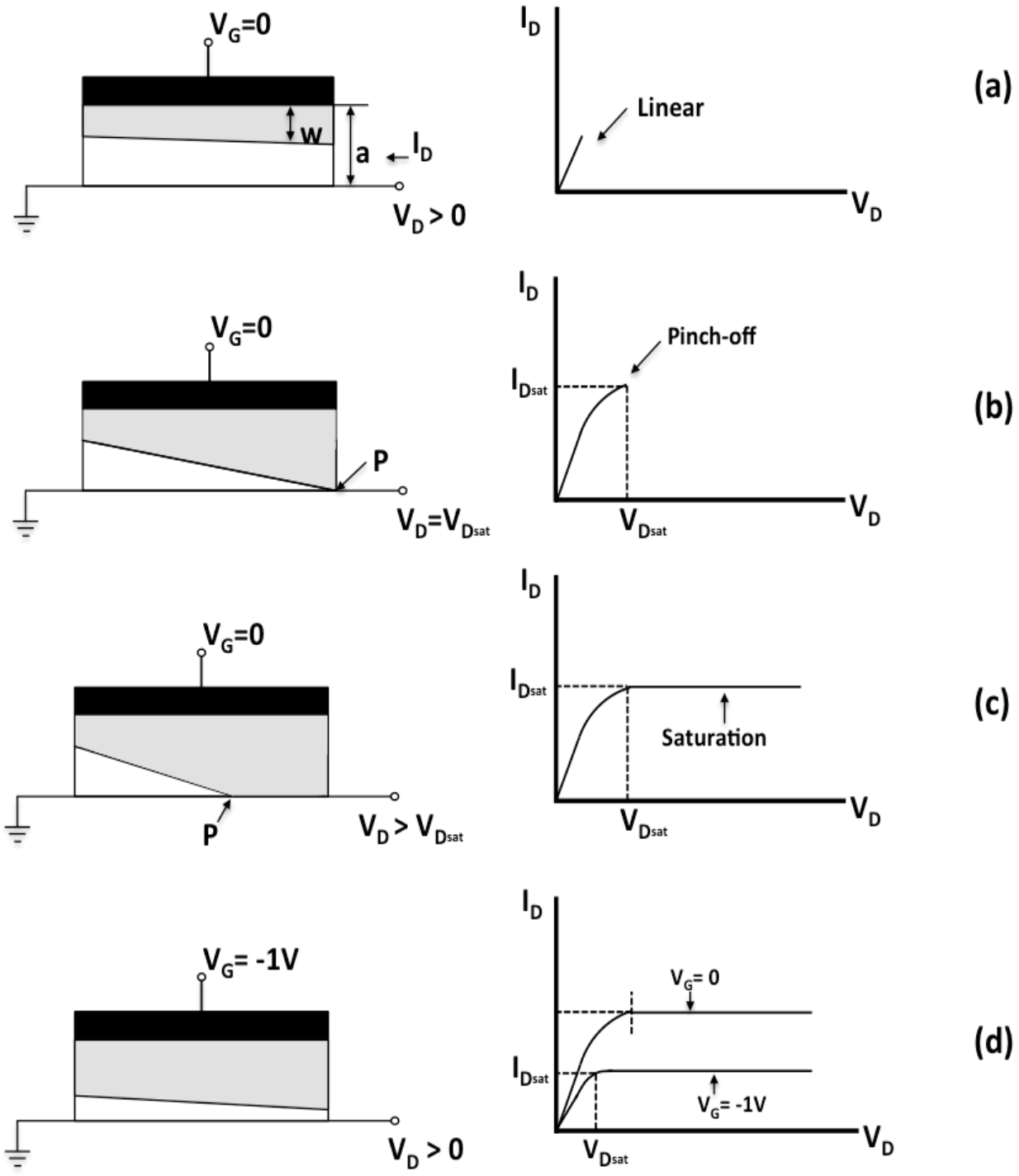

Figure 3.2 Variation of the depletion-layer width and output characteristics of a MESFET under various biasing conditions[28]

The IV curve, figure 3.3, shown below has been plotted by measuring I_d (drain current) with change of applied V_g (gate voltage) from 0 to -1V with increment of -0.25V.

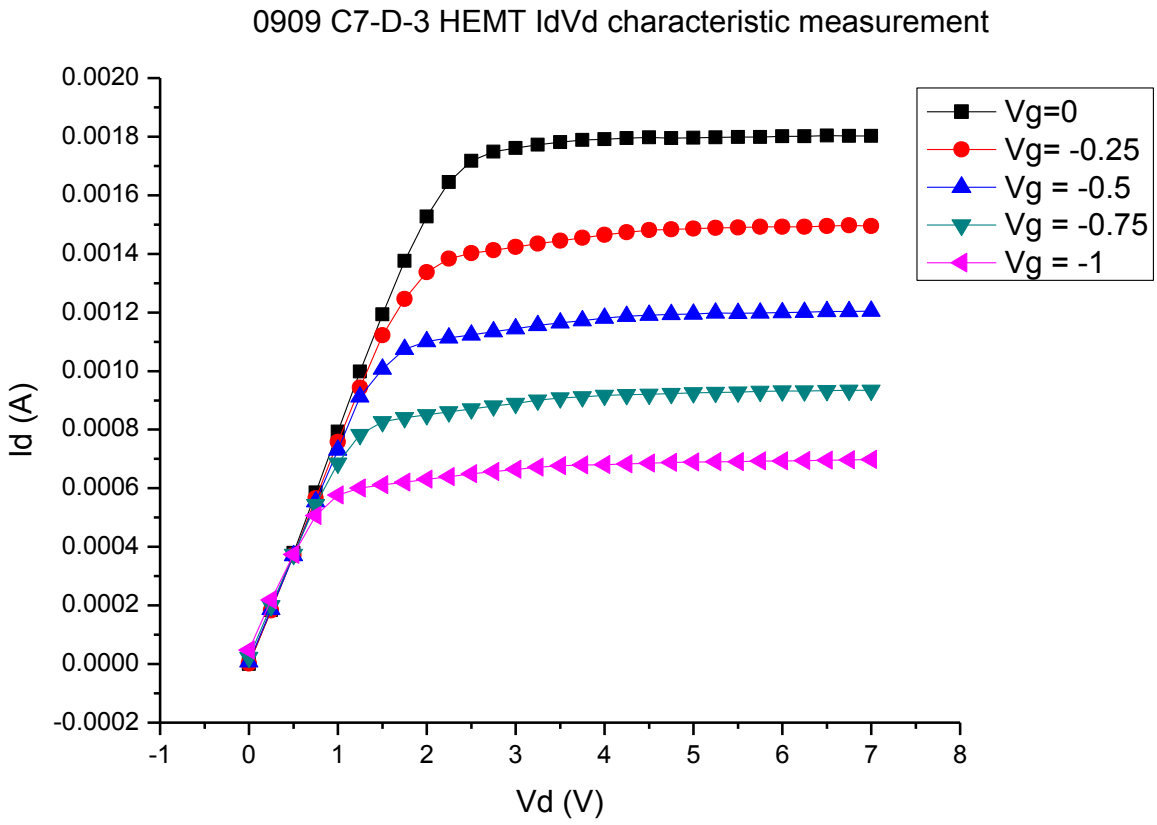

Figure 3.3 I_d-V_d measurement of HEMT by changing applied gate voltage

3.3 Capacitance-Voltage measurement

One of the conventional measurement techniques for semiconductor to characterize their electron carrier concentration profile is capacitance-voltage (C-V) curve measurement which shows the change of the capacitance with respect to voltage applied between the metal layer and insulating layer.[29] HEMT device which has both schottky metal contact and ohmic contact on the semi-insulating surface, called lateral structure, can consider semiconductor layer and the

schottky contact as two parallel plates of capacitor. Traditional capacitance voltage measurement can provide the thickness of oxide, threshold voltages, and also carrier density of the semiconductor device. The most critical feature of the HEMT capacitor is the variation of the capacitance with respect to the changing voltage applied on. Once the voltage is applied on the gate, the applied bias will induce the depleted charge area of width W in the semiconductor. The capacitance through the CV measurement can be described as below.

$$C = \frac{\varepsilon_0 \varepsilon_r A}{W} \quad \leftrightarrow \quad W = \frac{\varepsilon_0 \varepsilon_r A}{C}$$

where ε_0 is permittivity of free space, ε_r is relative permittivity, A is the area of the metal contact, and W is the width of space charge region. CV measurement is carried out with two probes one on the schottky contact and the other on the ohmic contact. The DC bias applied to gate enables the HEMT structure to experience two different modes, accumulation and depletion.

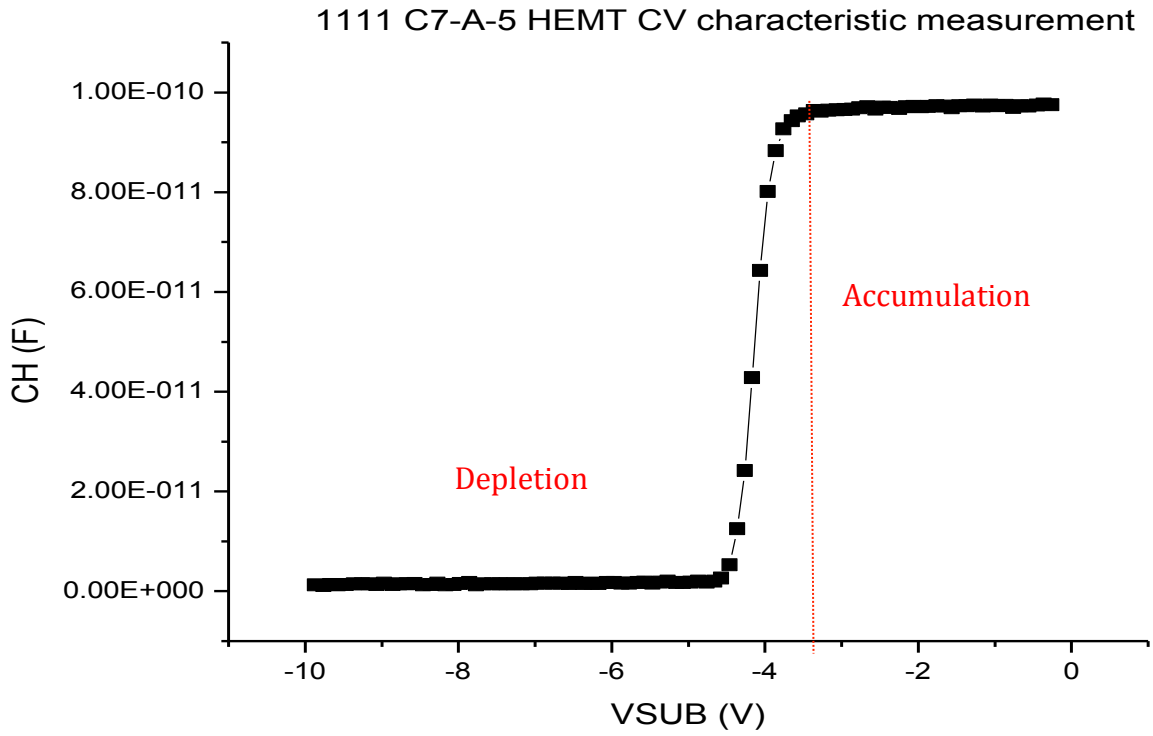

Figure 3.4 Capacitance voltage measurement

Figure 3.5 shows C-V measurement system used to conduct the measurement which is consisted of Keithley 595 Quasistatic CV meter, a Keithley 590 CV analyzer, a Keithley 230 voltage source and a shielded probe station.

Figure 3.5 Capacitance voltage measurement system

3.4 Summary

Conventional measurement technique, current-voltage and capacitance-voltage measurements, has been carried out with circular shape high electron mobility transistor in order to characterize electrical properties. I-V measurement shows pinch-off voltage and saturation current as a transistor, which mean it works as rectifier. C-V measurement tells that electrons existing in the two dimensional electron gas channel showing accumulation region without any voltage applied on the device.

Chapter Four

Photo current voltage measurement of AlGaN/GaN HEMT

4.1 Introduction

As a prospective electrical device, a high electron mobility transistor based on AlGaN/GaN has attracted noticeable interest of researchers and developers since it has unique and superior electrical properties due to the wide band gap energy (3.4eV), high breakdown voltage, stability, and other electrical properties.

As a conventional method of HEMT fabrication, GaAs has been adopted to use as semiconductor material of the device fabrication, however, due to its less efficient properties, gallium nitride has been used recently.

AlGaN/GaN HEMT structure is typically built up on a Si wafer because of its cost effectiveness. However, the lattice mismatch and different thermal expansion coeffiecients between Si and GaN, AlGAN/GaN has been considered carefully to reduce mismatch between GaN and Si, which is the main factor of defects inside multilayers.[30] Therefore, it is still a challenge, even though gallium nitride HEMT has remarkable electrical properties. In this chapter, the defect problems that AlGaN/GaN high electron mobility transistor has will be discussed and the unique and the simple spectroscopic photo current voltage technique to investigate the homogeneous defect distribution in the AlGaN/GaN high electron mobility transistor (HEMT) wafer.[31]

4.2 Current collapse

Despite the HEMT device showing rectifying property as a transistor through I-V measurement, we will be able to notice the reduced drain current after negative voltage is applied to the Schottky gate. This is the one of phenomena which reduces output drain current, called current collapse.

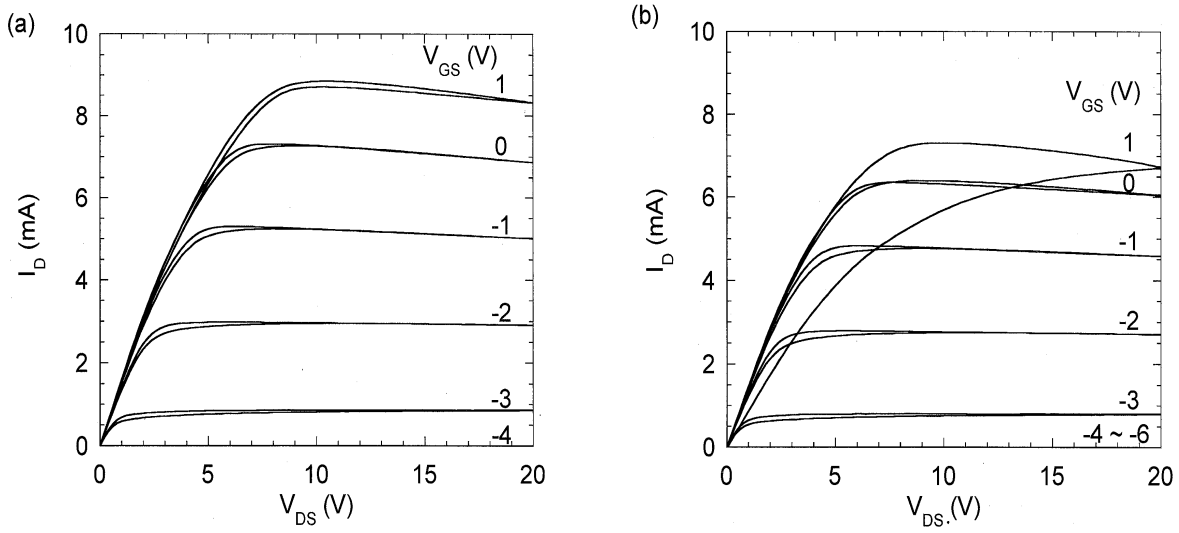

Figure 4.1 I_D-V_{DS} characteristics measured at gate voltage of (a) 1 to -4 V and (b) to -6 V[32]

As shown in the figure 4.1, the saturation drain current is decreased due to the trapping effect as negative voltage applied to the gate increases. The main factor inducing reduction of output drain current is defects existing inside multilayers, especially at the interface between gate metal and the barrier layer and bulk trap sites.[33,32] Once negative bias is applied to the Schottky gate, charge carriers from the gate will pass through the two-dimensional electron gas channel. However, due to the existence of defect sites mainly at the interface between Schottky and AlGaN barrier layer, electron charges will be trapped to defects. Therefore, it is of great importance to reduce the surface/interface and bulk traps that will reduce the number of charge carriers in the channel.

4.3 Photoionization

In order to study deep traps inside the multilayers of the HEMT device, a photoionization technique was performed. The mechanism of the photoionization technique is based on de-trapping of electron charges trapped at defects by illuminating light, which has higher energy than the threshold energy of the traps onto the HEMT device. Once trapped electrons obtain excess energy to jump up the threshold energy of the defects, electrons will get excited and be released from the defect sites. Therefore, excited electrons will drift back into the charge carrier channel. As a result, due to the increased number of the electrons in the channel, the drain current will be increased, and the total output power will be increased as well.

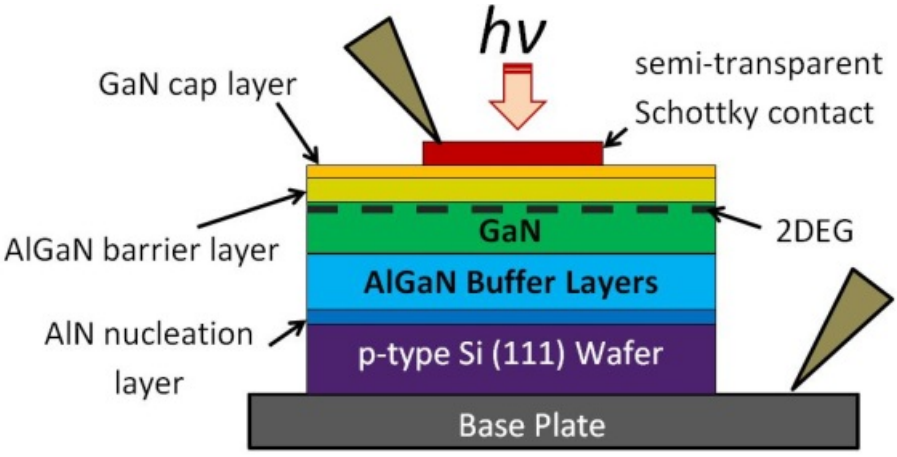

Figure 4.2 Schematic sample structure and configuration of photoionization measurement

4.4 Experiment and Photocurrent measurement

Epitaxial growth of HEMT layers has been conducted on 6 inch p-type Silicon wafer by MOCVD (Metal Organic Chemical Vapor Deposition) from the wafer manufacturer. The epi structure layers are in the following order: AlN nucleation layer (0.25 μm) on p-type silicon wafer, AlGaN buffer layers with different ratios of Aluminum composition from 20% and 75%, undoped GaN (1 μm), AlGaN barrier layers (20 nm), and lastly a GaN cap layer (2 nm).[33] The schematic HEMT structure is shown below in figure 4.3. The 6" silicon wafer for HEMT fabrication is diced into 1cm x 1cm size. Three Pieces of diced silicon wafer are chosen from three different regions, top, middle, and bottom.

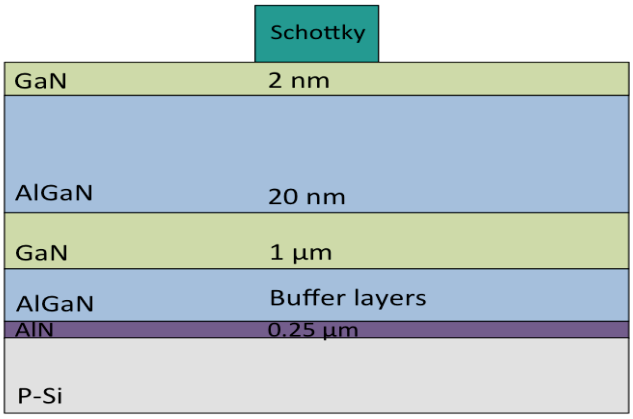

Figure 4.3 AlGaN/GaN HEMT structure on p-type Si substrate

Afterward, by using direct-current (DC) magnetron sputtering system, metal deposition with Ni is carried out to construct 600 μm diameter and 20nm thickness circular Schottky diode on the GaN cap layer. Then, photo current-voltage measurement has been conducted to investigate the effect of the illumination of the light onto the HEMT wafer. Schematic configuration of spectroscopy photo I-V measurement system shown in the figure 4.4 has been used to clarify deep traps in the AlGaN/GaN HEMT device. The photo I-V systems consist of Apex 150W

xenon lamp, a stepping motor controller, monochromator, a keithley 6487 pico-ammeter/voltage source, a micromanipulator and computer. The data collected from the computer by varying the wavelength of the light via monochromator with respect to the changing voltage started from -20 V to +5 V is demonstrated into spectroscopic photo I-V graphs. The photo current-voltage measurement was performed by sweeping different wavelengths from 800 nm to 400 nm (lower energy wavelength to higher energy wavelength). The main reason that I changed the wavelengths from longer to shorter is due to the persistent photoconductivity, which is predominant in HEMT structure.[34] Therefore, by changing wavelengths from longer to shorter (lower energy to higher energy), each different sweeping is not affected by remaining excited electrons or current after sweeping specific wavelength light.

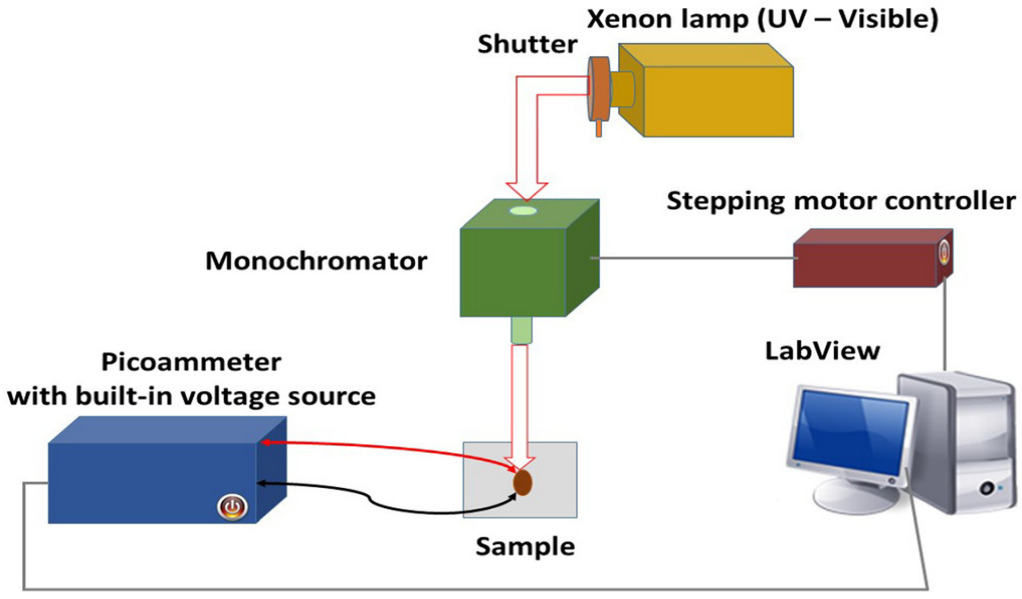

Figure 4.4 Schematic configuration of spectroscopic photo I-V measurement system[33]

Figure 4.5 shows spectroscopic photo current-voltage measurement in semi-log scale from three different regions of the 6" silicon wafer, (a) is picked from the top, (b) is from the middle, and

(c) is from the bottom part. Each plotted graph shows that it has the maximum value of the current corresponding to the specific wavelength and also the measured current does not reach the maximum value with the strongest wavelength. This shows that there are electrons trapped by defects, which have specific threshold energy in the HEMT multilayers, and also if the illuminated light has enough energy corresponding to the threshold energy of the defects, the trapped electrons can be excited.

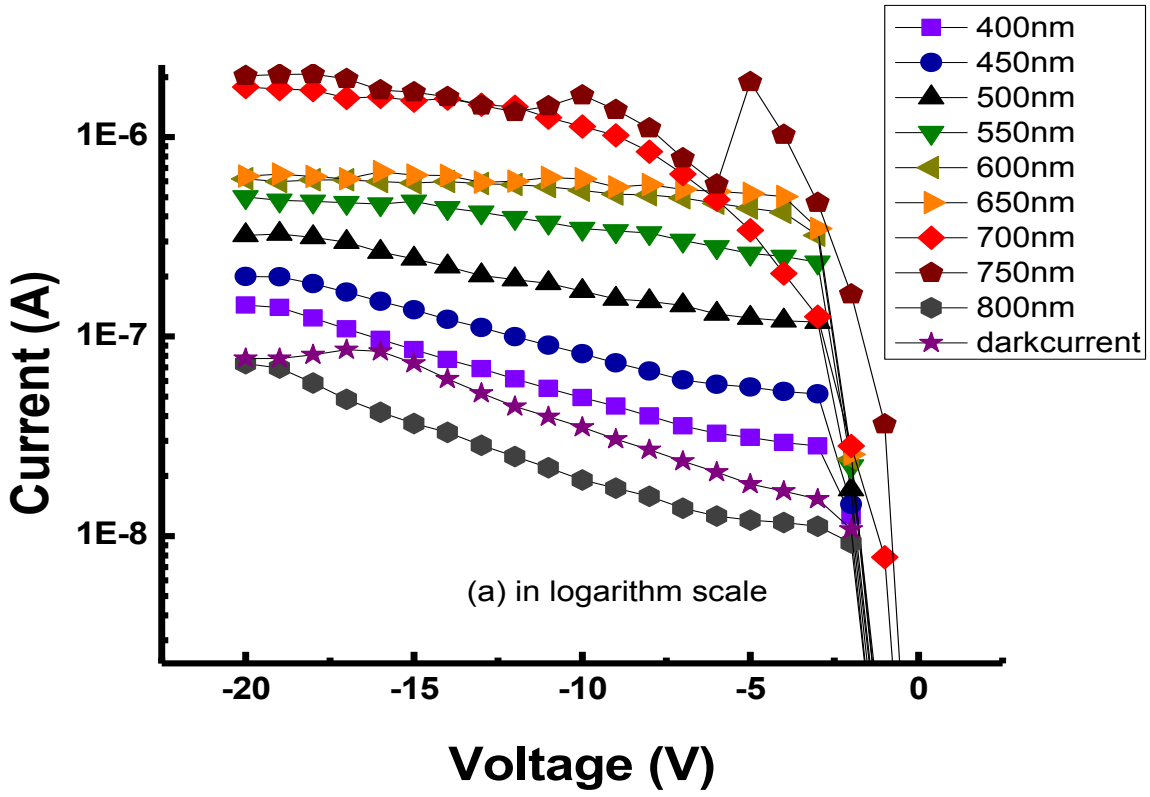

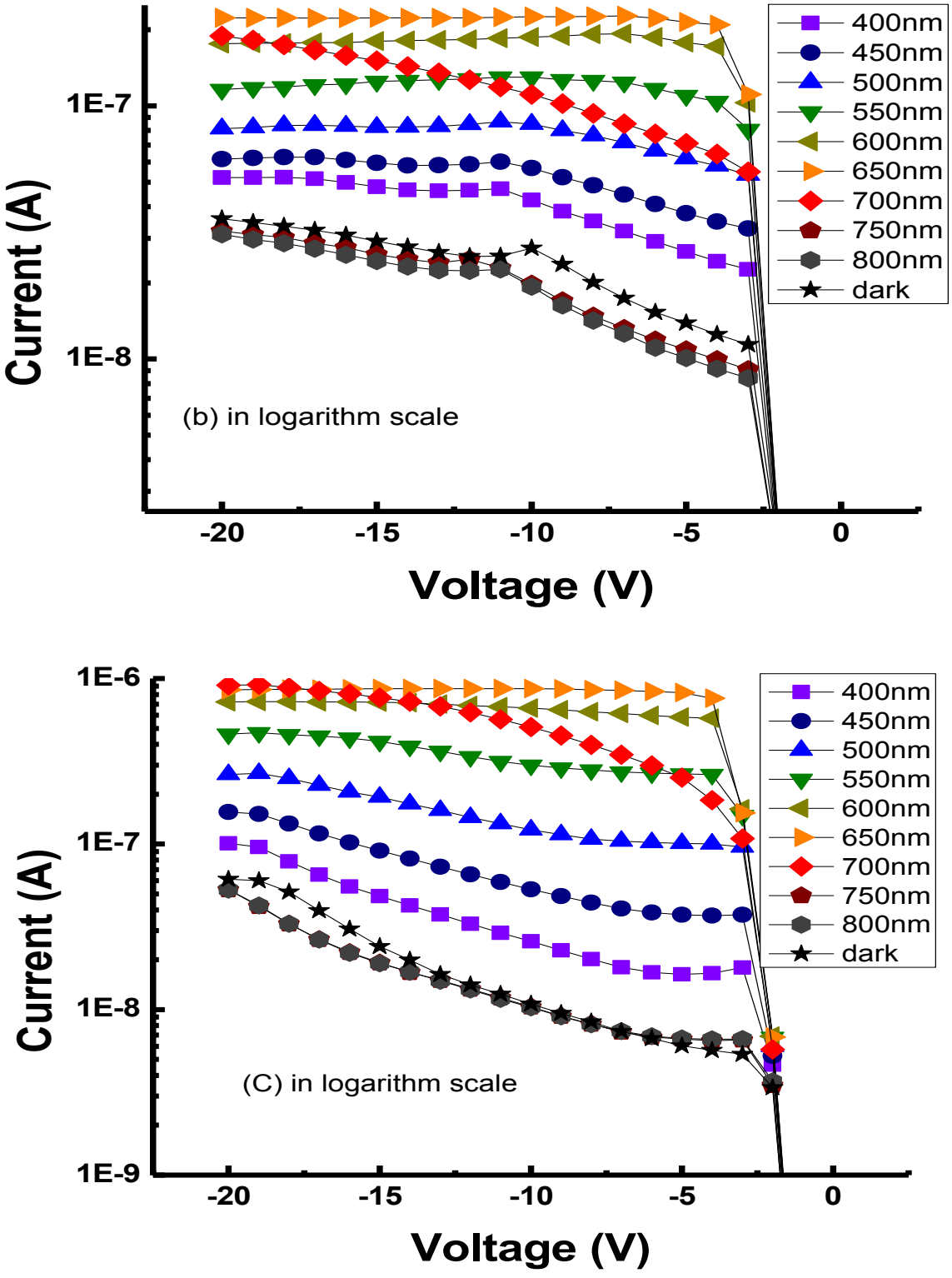

Figure 4.5 Spectroscopic photo I-V measurement with respect to different wavelengtgh (a) is from the top, (b) is from middle, and (c) is from bottom

4.5 Results and discussion

The samples from three different regions have been measured by the photo current-voltage system. For the top sample, the maximum photocurrent has been measured when light with the wavelength 750nm is illuminated, and then decreases as the wavelength is decreased from 700 nm to 400 nm. For the center and bottom samples, they have been excited under the light with 700 nm wavelength and have the maximum photocurrent at 650 nm wavelength. Then, the photocurrent weakened as the strength of the light increased. It can be interpreted as some specific response of the photo I-V graphs might be associated with threshold energy of defects inside the heterostructure and an important factor to identify the defects.

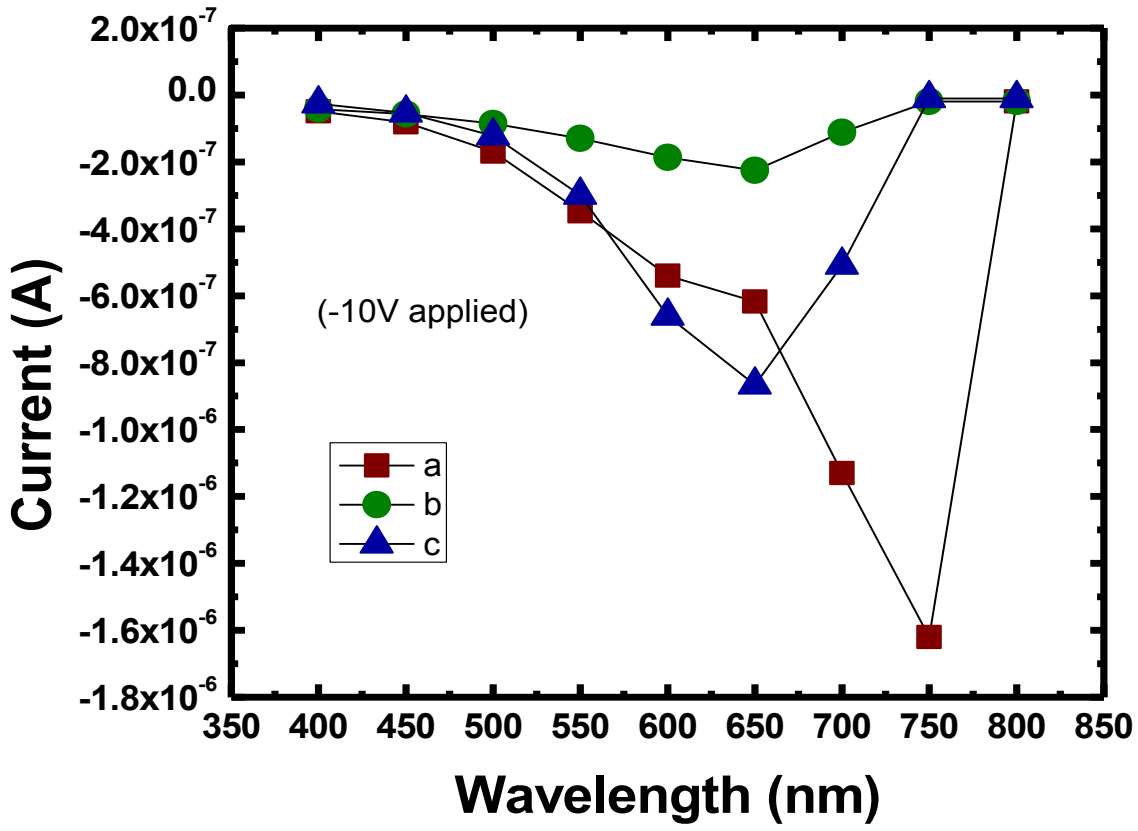

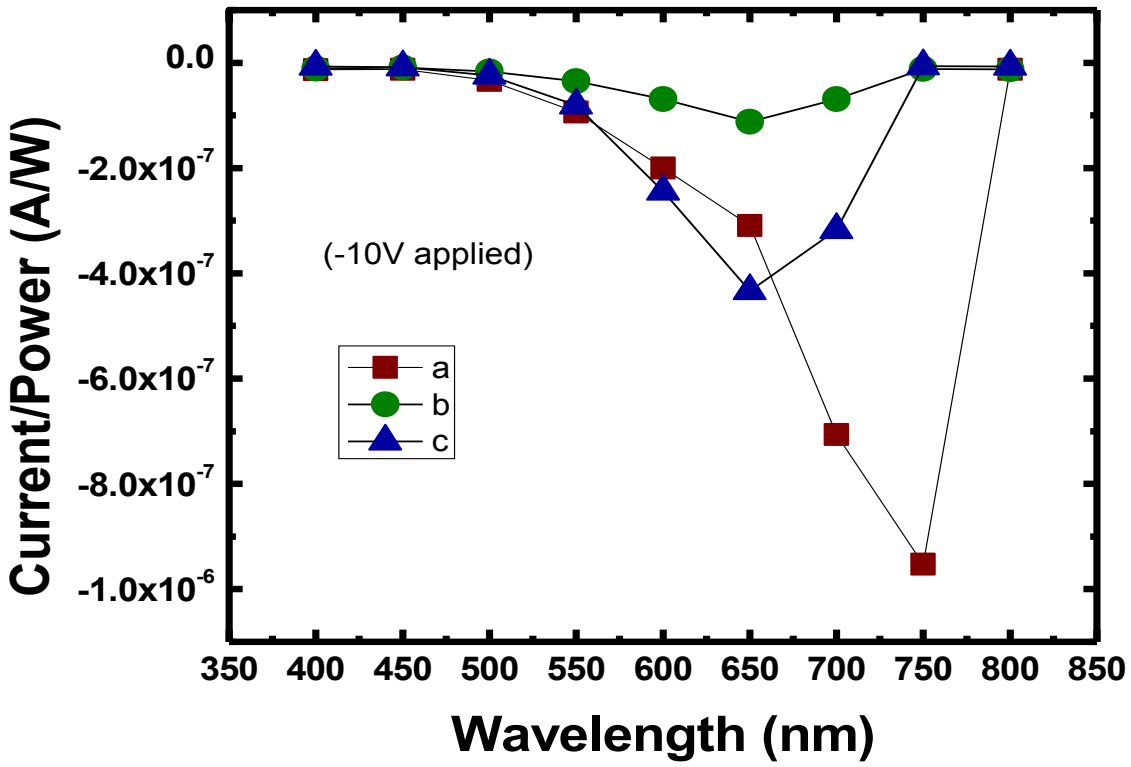
0.0
-2.0x10-7
-4.0x10-7
-6.0x10-7
-8.0x10-7
-1.0x10-6
Current/Power (A/W)
(-10V applied)
a
b
c
350 400 450 500 550 600 650 700 750 800 850
Wavelength (nm)

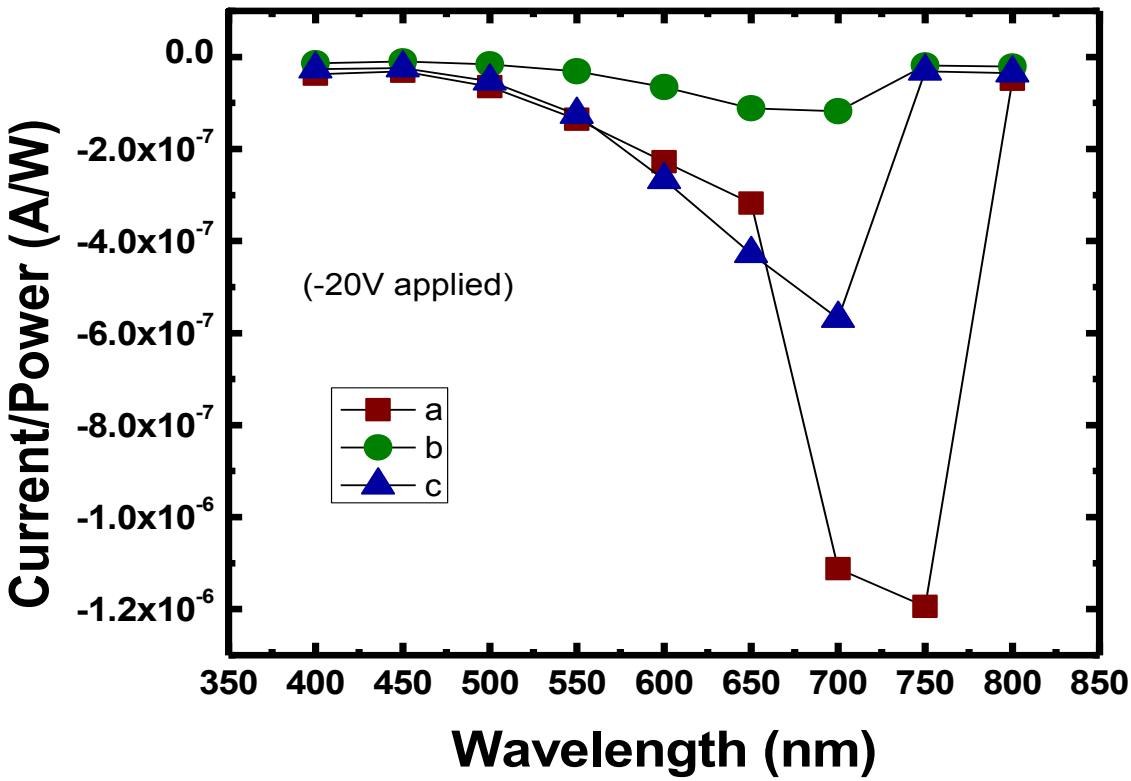
0.0
-2.0x10-7
-4.0x10-7
-6.0x10-7
-8.0x10-7
-1.0x10-6
-1.2x10-6
Current/Power (A/W)
(-20V applied)
a
b
c
350 400 450 500 550 600 650 700 750 800 850
Wavelength (nm)

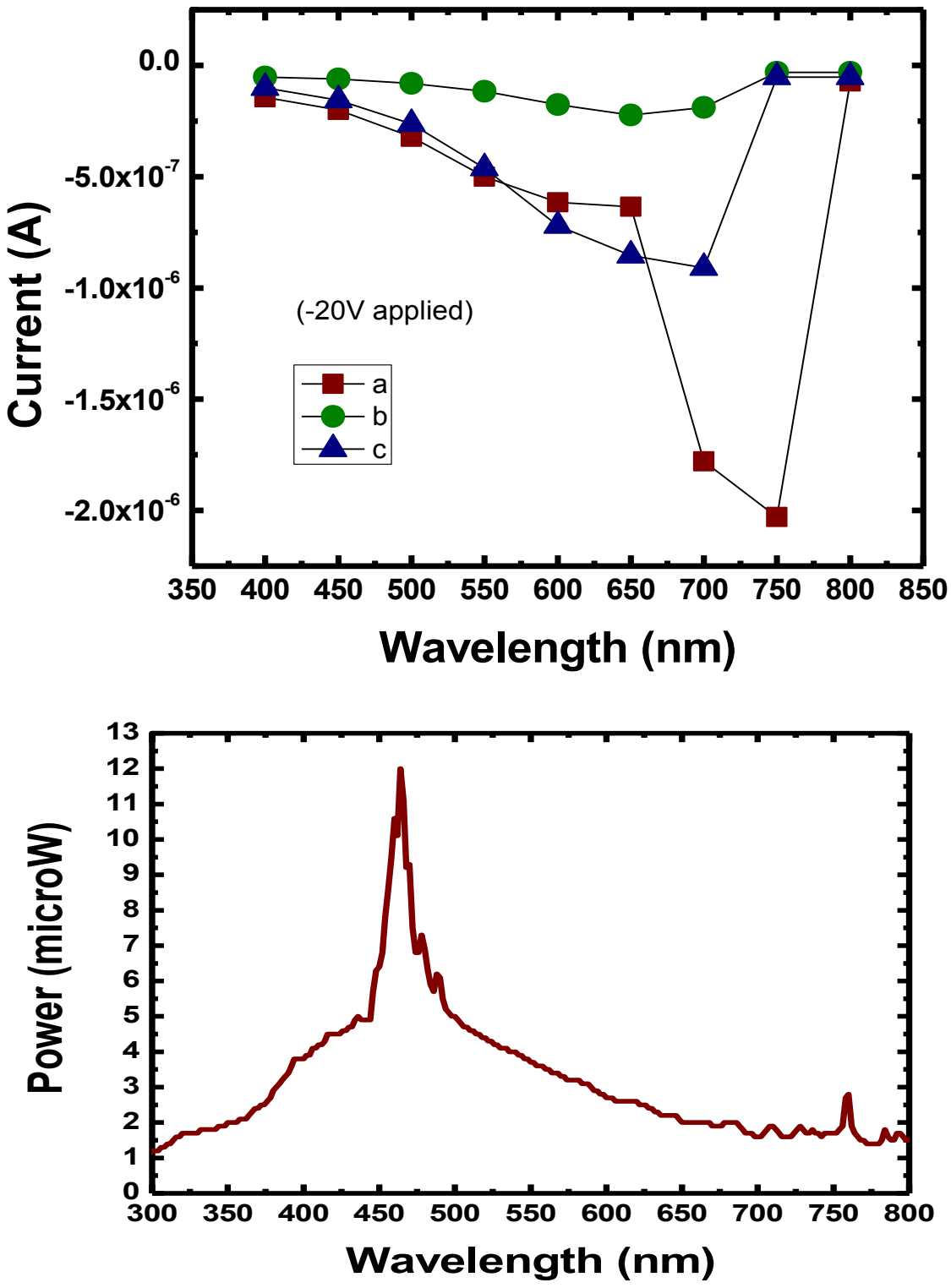

Figure 4.6 current vs wavelength graphs with two different voltages applied on, and Responsivity (current/power intensity of wavelength) vs Wavelength graphs of three different samples with different voltages applied on.

Figure 4.6 shows responsivity (current/each wavelength power) vs wavelength of three different samples. As we measured the photo current-voltage characteristics, there is obvious propensity with respect to the change of wavelength. However, due to the existence of the power intensity of light itself from the light source that we shine on our sample, they might be able to affect the result at the end. In order to avoid the effect of power of light, we have normalized the current values by dividing them by power intensity of corresponding wavelengths. As a result, the responsivity (normalized current) appears similarly as before, which tells that the variation of the current value with respect to the wavelength is not influenced by the power of light itself, but the excitation of the trapped electrons from the defects by illuminating the samples. Finally, it seems the electron excitations are generated by the corresponding wavelength, which has enough energy to overcome the threshold energy to eject the electrons from the defects.

4.6 Summary and conclusions

Spectroscopic photo I-V measurement technique has been proposed and applied to the 6" GaN HEMT wafer. Comparing to other photocurrent-voltage measurements technique, the measurement method introduced in this thesis has an advantage that we can chose specific wavelength of light. As a result, collected data tells more precise results to investigate defect identifications. The variation of the photo I-V measurement depending on the different wavelength light indicates that defects across the wafer have different distributions and type of defects. Therefore, proposed spectroscopic photo I-V method can be useful to diagnose the electrical homogeneity of GaN HEMT wafer with minimum preparation steps.

Chapter Five

Breakdown voltage measurement and analysis

5.1 Introduction

It has been a huge attraction to wide band gap semiconductor materials for various electrical applications especially in power electronic devices. AlGaN/GaN based HEMT has been considered as a prospective device due to their exceptional material properties under harsh conditions, for instance, high temperature, high pressure, and high voltage power. Even though AlGaN/GaN HEMT has superior electrical properties, one issue has been pointed out that it has a relatively large leakage current. Due to the large leakage, abrupt increase of current might be observed from the HEMT devices after breakdown. Thus, it is crucial to investigate fundamental mechanisms which restrict the breakdown voltage and associated solution in order to enhance the electrical properties of AlGaN/GaN HEMT. In this chapter, breakdown mechanism, various factors that affect the breakdown voltage, and area dependent of breakdown voltage measurement of ohmic contact on the AlGaN/GaN based wafer will be mainly discussed.

5.2 Breakdown phenomenon and measurement

Breakdown voltage is an electrical parameter that defines the maximum electrical voltage that can be applied on the device until it collapses. Major experiments about HEMT have focused on explaining and enhancing the breakdown field strength in order to obtain better electrical properties. Usually atoms within insulators posses quite strongly bound electrons, resisting free electrons. However, it is not always possible for insulators to resist infinite magnitude of voltage applied on them. If there is an enormous voltage operating on any type of materials, even insulators, they will be overwhelmed by high voltage and eventually electric current flow will occur. Unlike a conductor, which shows linearly increasing current with respect to the voltage applied on it, current through an insulator displays non-linear aspect. Voltage below the threshold cannot generate current flow through insulators, however, if the voltage exceeds the specific voltage level there will be current. After electric current is allowed to flow inside of insulators by enough voltage applied, there will be breakdown behavior.

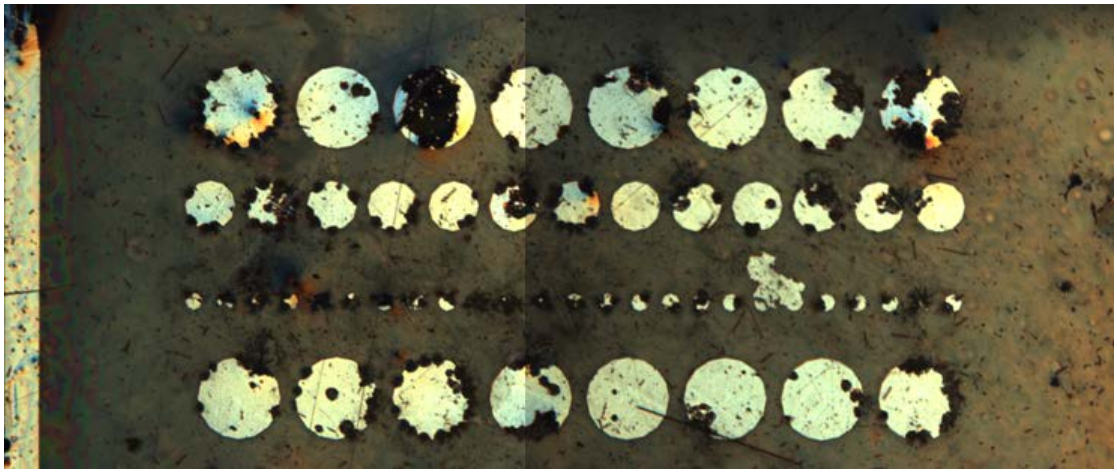

Figure 5.1 Schottky diode after breakdown

The commencement of breakdown of AlGaN/GaN high electron mobility transistor or other FETs (Field Effect transistor) can be caused by impact ionization. It has been studied that if there is a strong electric field applied to a device, the injected electrons from the source obtain enough kinetic energy due to the strong electric field so they can excite other bound electrons, resulting in generation of electron-hole pairs consequently through the GaN buffer layer. This continuous process is also so called an avalanche process. Once electrons get excited, the released electrons can excite other bound electrons due to the strong electric field applied to the device. Released electrons can pass through the buffer layer and this is the main factor of leakage current and device breakdown.

In addition, a punchthrough effect can be a secondary factor of breakdown. When there is electric current flow underneath the depletion region of the gate that goes through the non-conductive buffer layer, it is a so called punchthrough effect. Punchthrough effect produces increase of drain leakage current and this leakage current is normally considered as an initiator of device breakdown.[35] In order to enhance the breakdown voltage, the punchthrough is necessary to be prevented by introducing *p-type* doping such as carbon or Fe into the buffer layer to generate acceptor like donors in the GaN buffer layer so that the electrons can be trapped.[36] Even though carbon doping into the buffer layer reduces the leakage current through the buffer layer, it has issues such as the acceptor behaving as defects, rapid increase of R_{on} in the device, and the reduction of saturation drain current. The other method to reduce the punchthrough effect is to block the leakage current through the buffer layer by using double heterostructure buffer layer or by controlling the thickness of the buffer layer.[37] The GaN buffer layer requires lots of care to obtain less dislocation density and lattice mismatch. With the help of suitable growth technique, the thickness dependent breakdown voltage is demonstrated in the figure 5.2.

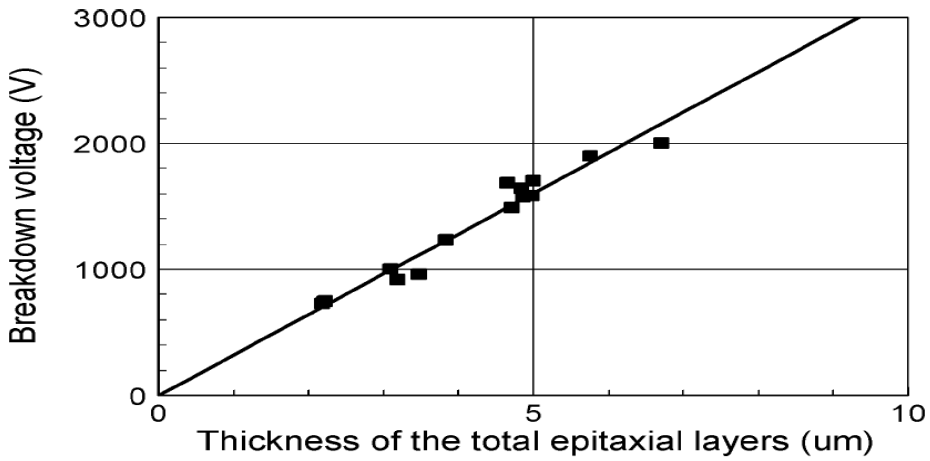

Figure 5.2 Dependence of breakdown voltage on total epitaxial layer thickness[38]

In addition to the thickness of the buffer layer, it has been pointed out that the device size is also considered as a factor that can vary the breakdown voltage. We have fabricated and measured breakdown voltage of Schottky contact in different diameters as shown in the figure 5.3, 150μm(left), 300μm(middle), and 600μm(right).

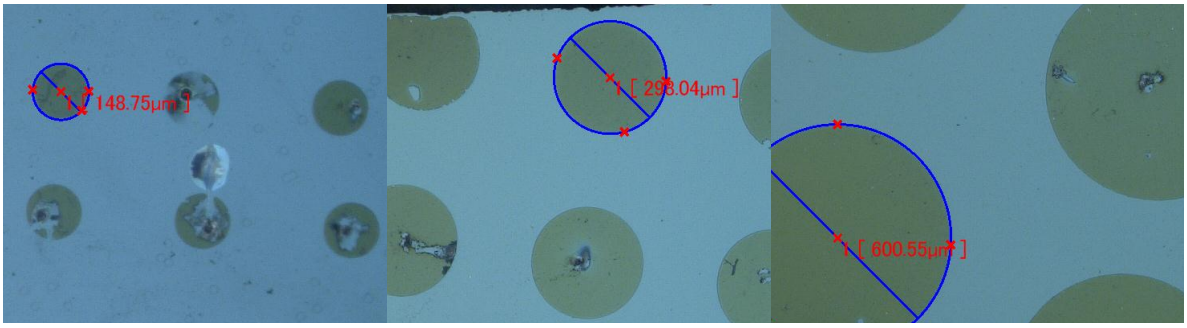

Figure 5.3 Breakdown measurement of different diameter Schottky didoes

It has been indicated by Iruthayaraj *et al.* that the vertical breakdown measurement depends on the thickness of buffer layers, and also the breakdown voltage decreases as the device area

increases.[39] The breakdown voltage measurement is conducted with three different sizes of devices, and it is shown in figure 5.4 and table 5.1 and table 5.2

ohmic to ohmic		150µm (-)→(+)	300µm (-)→(+)	600µm (-)→(+)		150µm (+)→(-)	300µm (+)→(-)	600µm (+)→(-)
V_{Break} (V)	1	780	690	680		-690	-800	-700
	2	400	730	700		-700	-315	-480
	3	700	500	400		-490	-660	-600
	4	500	600	575		N/A	-585	-300
	5	N/A	525	400		N/A	N/A	N/A
Mean (V)		**595.00**	**609.00**	**551.00**		**-626.67**	**-590.00**	**-520.00**
STDEV (V)		**175.40**	**100.27**	**145.79**		**118.46**	**203.84**	**172.05**

Table 5.1 Average breakdown measurement and standard deviation with different sizes and sweeping direction (a)

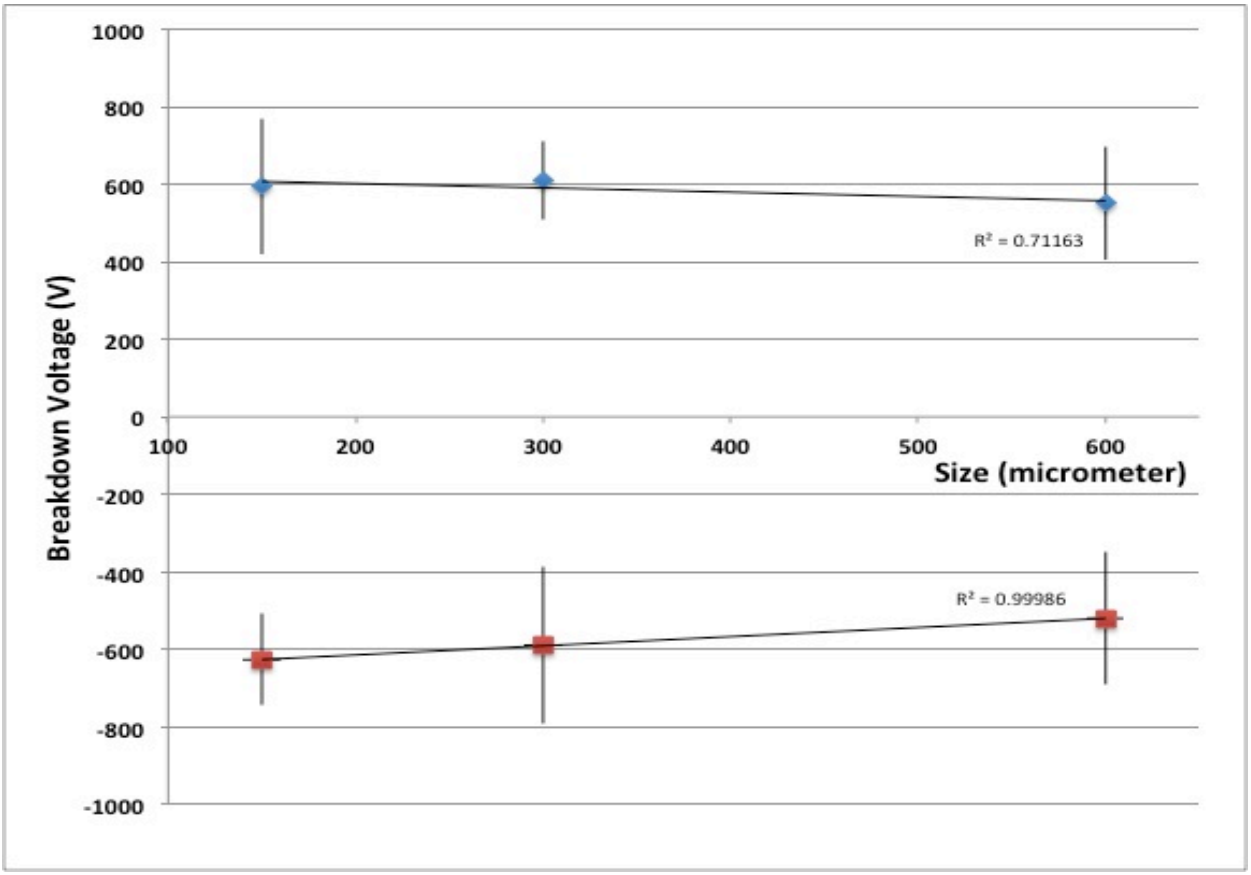

Figure 5.4 Breakdown voltage with different sizes and sweeping directions measured from ohmic to ohmic contact (a)

ohmic to bottom		150µm	300µm	600µm		150µm	300µm	600µm
		(-)→(+)	(-)→(+)	(-)→(+)		(+)→(-)	(+)→(-)	(+)→(-)
V_{Break} (V)	1	500	720	420		-850	-740	-750
	2	700	830	500		-800	-800	-300
	3	475	820	440		-400	-800	-500
	4	800	370	535		-480	-280	-500
	5	280	280	480		N/A	N/A	-250
	6	N/A	N/A	560		N/A	N/A	N/A
	7	N/A	N/A	400		N/A	N/A	N/A
	8	N/A	N/A	400		N/A	N/A	N/A
Mean (V)		**551.00**	**604.00**	**466.88**		**-632.50**	**-655.00**	**-460.00**
STDEV (V)		**203.73**	**260.25**	**61.47**		**225.59**	**251.59**	**198.12**

Table 5.1 Average breakdown measurement and standard deviation with different sizes and sweeping direction (b)

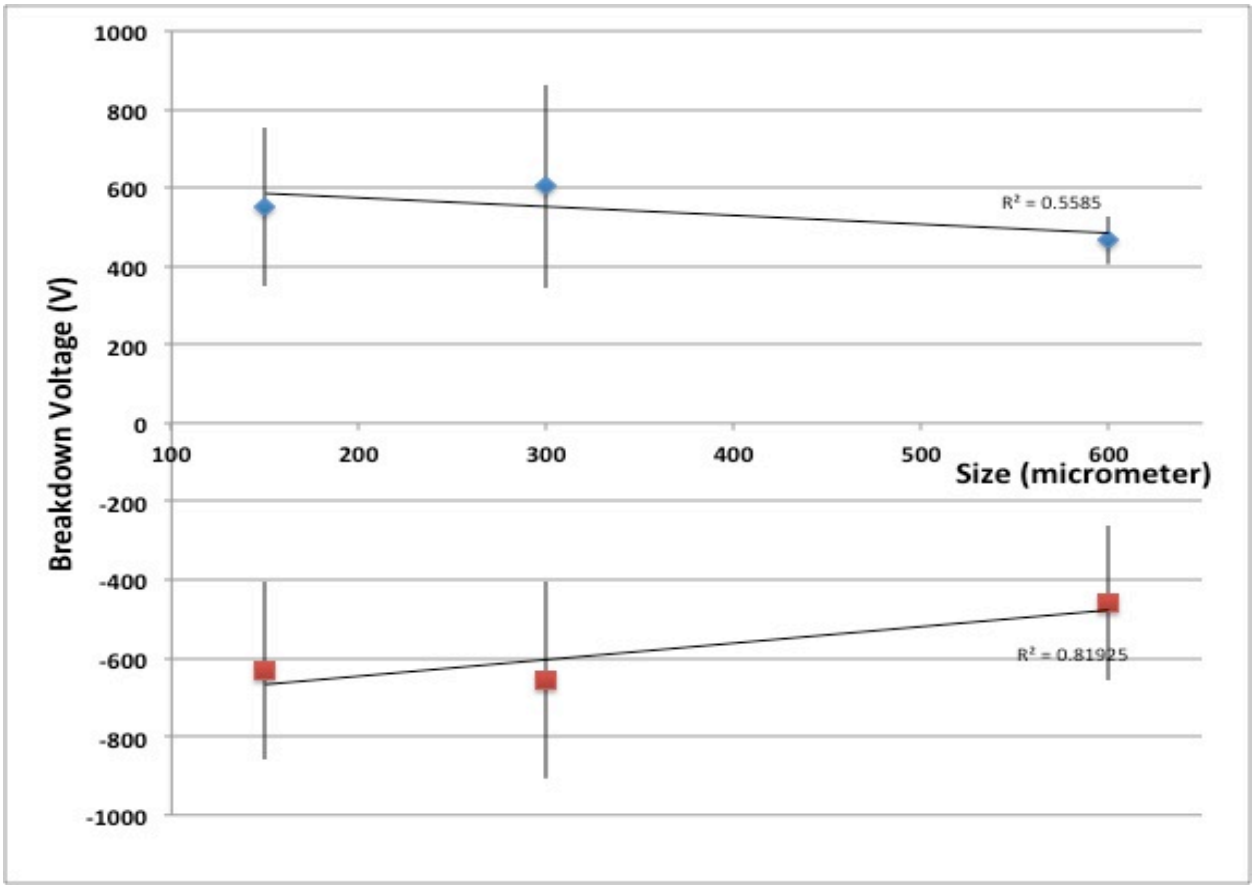

Figure 5.4 Breakdown voltage with different sizes and sweeping directions measured from ohmic to bottom (b)

In order to analyze the tendency of the breakdown voltage with different device sizes, the raw data of breakdown measurement has been statistically used to get an average and standard deviation as shown in the table 5.1 and figure 5.4 above. It shows a tendency that indicates decreasing breakdown voltage by increasing the size of the device.

5.3 Conclusion

Our study shows that leakage current caused by injected electrons to the source and the impact ionization are able to induce the electric breakdown to the device. Also, the punchthrough effect can be a secondary factor that may induce the device breakdown, depending on device configurations. Based on the individual data with different sizes of the devices we measured and analyzed statistically, it shows a tendency to have lower breakdown voltage characteristics with smaller size of the device. It is because of the higher possibility of defects that exist at the surface or the interface of larger devices.

Reference

[1] F. Benkabou (a), P. Becker (b), M. Certier (c), and H. Aourag "Structural and Dynamical Properties of Zincblende GaN" phys. stat. sol. (b) 209, 223 (1998)

[2] H. Morkoç, *Nitride Semiconductors and Devices,* pp.**8** (Springer, Berlin, 1999)

[3] X. M. Zhang, R.S. Ma, X.C Liu, "Topological insulators with unexpectedly HgTe-like band inversion in hexagonal wurtzite-type binary compounds" EPL, pp.**2** 103 (2013)

[4] S.J. Pearton, F. Ren, A.P. Zhang, K.P. Lee, "Fabrication and performance of GaN electronic devices" Materials Science and Engineering, pp.**2-3** R30 (2000)

[5] Rüdiger quay, "Gallium Nitride Electronics", pp**21** (Springer)

[6] Rathnait D.Long, Paul C. McIntyre "Surface Preparation and deposited Gate Oxides for Gallium Nitride Based Metal oxide Semiconductor Devices" Materials. **5**,1297-1335 (2012)

[7] N.Nepal, J. Li, "temperature and compositional dependence of the energy band gap of AlGaN alloys" Appl. Phys. **87**, 242105 (2005)

[8] Fabio Sacconi, Aldo Di Carlo, P. Lugli, and Hadis Morkoc, "Spontaneous and Piezoelectric Polarization Effects on the output Characteristics of AlGaN/GaN Heterojunction Modulation Doped FETs" IEEE Vol.**48** (2001)

[9] O. Ambacher, B. Foutz, J. Smart, J. R. Shealy N. G. Weimann, K. Chu, M. Murphy, A. J. Sierakowski, W. J. Schaff, and L. F Eastman, "Two dimensional electron gases induced by spontaneous and piezoelectric polarization in undoped and doped AlGaN/GaN heterostructures", Journal of Appl. Phys. **87,** 334 (2000)

[10] S.H. Park, "Spontaneous polarization effects on electronic and optical properties of wurtzite GaN/AlGaN quantum well lasers" Journal of the Korean Phys. Society. **38** (2001)

[11] E. T. Yu, X. Z. Dang, P. M. Asbeck, and S. S. Lau, "Spontaneous and piezoelectric polarization effects in III-V nitride heterostructures", Journal of Vacuum Science & Technology B 17, 1742 (1999)

[12] Oded Katz, Student Members, IEEE, Adi Horn, G. Bahir, and Joseph Salzman, "Electron Mobility in an AlGaN/GaN Two-Dimensional Electron Gas I-Carrier Concentration Dependent Mobility" IEEE, Vol **50** (2003)

[13] P. B. Klein, S. C. Binari, K. Ikossi, A. E. Wickenden, D. D. Koleske, and R. L. Henry "Current collapse and the role of carbon in AlGaN/GaN high electronmobility transistors grown by metalorganic vapor-phase epitaxy", Appl. Phys. **79**, 21 (2001)

[14] P.B. Klein, "Photoionization spectroscopy in AlGaN/GaN high electron mobility transistors", Journal of Appl. Phys. **92,** 9 (2002)

[15] P. B. Klein, S. C. Binari, "Photoionization spectroscopy of deep defects responsible for current collapse in nitride-based field effect transistors" J. Phys. Condens. Matter **15** R1641 (2003)

[16] N Chaturvedi, U Zeimer, JW¨urfl and G Tr¨ankle , "Mechanism of ohmic contact formation in AlGaN/GaN high electron mobility transistors", Semicond. Sci. Technol. **21,** 175–179 (2006)

[17] B. Van Daele, G. Van Tendeloo, W. Ruythooren, J. Derluyn, M. R. Leys, and M. Germain, "The role of Al on Ohmic contact formation on n -type GaN and AlGaN GaN", Applied Physics Letters 87, 061905 (2005)

[18] N. A. Papanicolaou, M. V. Rao, J. Mittereder, and W. T. Anderson, "Reliable Ti/Al and Ti/Al/Ni/Au ohmic contacts to n-type GaN formed by vacuum annealing", Journal of Vacuum Science & Technology B 19, 261 (2001)

[19] Abhishek Motayed, Ravi Bathe, Mark C. Wood, Ousmane S. Diouf, R. D. Vispute, and S. Noor Mohammad, "Electrical, thermal, and microstructural characteristics of Ti/Al/Ti/Au multilayer Ohmic contacts to n -type GaN", Journal of Applied Physics 93, 1087 (2003)

[20] http://web.tiscali.it/decartes/phd_html/node3.html

[21] Salah Saadaoui a), Mohamed Mongi Ben Salem a), Malek Gassoumi, Hassen Maaref, and Christophe Gaquie`re, "Electrical characterization of (Ni/Au)/Al0.25Ga0.75N/GaN/SiC Schottky barrier diode" JOURNAL OF APPLIED PHYSICS 110, 013701 (2011)

[22] H. Zhang, E. J. Miller, and E. T. Yu, "Analysis of leakage current mechanisms in Schottky contacts to GaN and Al0.25Ga0.75N/GaN grown by molecular-beam epitaxy", JOURNAL OF APPLIED PHYSICS **99**, 023703 (2006)

[23] Engin Arslan,a) Serkan Bütün, and Ekmel Ozbay, "Leakage current by Frenkel–Poole emission in Ni/Au Schottky contacts on Al0.83In0.17N/AlN/GaN heterostructures", APPLIED PHYSICS LETTERS 94, 142106 (2009)

[24] N. Miura a,*, T. Nanjo a, M. Suita a, T. Oishi a, Y. Abe a, T. Ozeki a, H. Ishikawa b, T. Egawa b, T. Jimbo b, "Thermal annealing effects on Ni/Au based Schottky contacts on n-GaN and AlGaN/GaN with insertion of high work function metal", Solid-State Electronics, Volume 48, Issue 5, (2004), Pages 689–695

[25] Lin Fang a), Shen Bo a)† , Lu Li-Wu a) , Ma Nan a), Xu Fu-Jun a), Miao Zhen-Lin a) , Song Jie a), Liu Xin-Yu b), Wei Ke b), and Huang Jun b), "Performance comparison of Pt/Au and Ni/Au Schottky contacts on AlxGa1−x N/GaN heterostructures at high temperature", Chin. Phys. B Vol. 19, No. 12 (2010)

[26] Fernando González-Posadaa, Jennifer A. Bardwellb, Simona Moisab, Soufien Haffouzb, Haipeng Tangb, Alejandro F. Brañaa, Elías Muñoza, "Surface cleaning and preparation in AlGaN/GaN-based HEMT processing as assessed by X-ray photoelectron spectroscopy" Applied Surface Science, Volume 253, Issue 14, 15 May 2007, Pages 6185–6190

[27] Douglas James Macfarlane "Design and fabrication of AlGaN/GaN HEMTs with high breakdown voltages"

[28] S.M. Sze "semiconductor devices physics and technology" 2nd edition

[29] Fang Lu, Dawei Gong, Jianbao Wang, Qinhua Wang, Henghui Sun, and Xun Wang, "Capacitance-voltage characteristics of a Schottky junction containing SiGe/Si quantum wells", Physical review B voltum 53, number 8 Feb 1996-II

[30] D Seghier and H P Gislason,"Characterization of photoconductivity in AlxGa1−xN materials", J. Phys. D: Appl. Phys. 42 (2009) 095103 (4pp)

[31] F. Tong, K. Yapabandara, C.-W. Yang, M. Khanal, C. Jiao,M. Goforth, B. Ozden, A. Ahyi, M. Hamilton, G. Niu,D.A. Ewoldt, G. Chung and M. Park , "Spectroscopic photo I – V diagnostics of nitride-based high electron mobilitytransistor structures on Si wafers", ELECTRONICS LETTERS 21st November 2013 Vol. 49 No. 24 pp. 1547 – 1548

[32] Takashi Mizutani, Senior Member, IEEE, Yutaka Ohno, M. Akita, Shigeru Kishimoto, and Koichi Maezawa, Member, "A Study on Current Collapse in AlGaN/GaN HEMTs Induced by Bias Stress", IEEE TRANSACTIONS ON ELECTRON DEVICES, VOL. 50, NO. 10, OCTOBER 2003

[33] Burcu Ozden, Chungman Yang, Fei Tong, Min P. Khanal, Vahid Mirkhani, Mobbassar Hassan Sk, Ayayi Claude Ahyi, and Minseo Park, "Depth-resolved ultra-violet spectroscopic photo current-voltage measurements for the analysis of AlGaN/GaN high electron mobility transistor epilayer deposited on Si", APPLIED PHYSICS LETTERS 105, 172105 (2014)

[34] Dang, X.Z., Wang, C.D., Yu, E.T., Boutros, K.S., and Redwing, J.M.: ' Persistent photoconductivity and defect levels in n-type AlGaN/GaNheterostructures ' , Appl. Phys. Lett. , 1998, 72 , pp. 2745 – 2747

[35] Eldad Bahat-Treidel, Oliver Hilt, Frank Brunner, Joachim Würfl, and Günther Tränkle, "Punchthrough-Voltage Enhancement of AlGaN/GaN HEMTs Using AlGaN Double-Heterojunction Confinement", IEEE TRANSACTIONS ON ELECTRON DEVICES, VOL. 55, NO. 12, DECEMBER 2008

[36] Maojun Wang and Kevin J. Chen, Senior Member, IEEE, "Improvement of the Off-State Breakdown Voltage With Fluorine Ion Implantation in AlGaN/GaN HEMTs", IEEE TRANSACTIONS ON ELECTRON DEVICES, VOL. 58, NO. 2, FEBRUARY 2011

[37] Eldad Bahat-Treidel, Frank Brunner, Oliver Hilt, Eunjung Cho, Joachim Würfl, and Günther Tränkle, "AlGaN/GaN/GaN:C Back-Barrier HFETs With Breakdown Voltage of Over 1 kV and Low $R_{ON} \times A$", IEEE TRANSACTIONS ON ELECTRON DEVICES, VOL. 57, NO. 11, NOVEMBER 2010

[38] Nariaki Ikeda, Yuki Niiyama, Hiroshi Kambayashi, Yoshihiro Sato, Takehiko Nomura, Member IEEE, Sadahiro Kato, and Seikoh Yoshida, "GaN Power Transistors on Si Substrates for Switching Applications" Proceedings of The IEEE - PIEEE , vol. 98, no. 7, pp. 1151-1161, 2010

[39] Iruthayaraj Beaula Rowena, Susai Lawrence Selvaraj, and Takashi Egawa, "Buffer Thickness Contribution to Suppress Vertical Leakage Current With High Breakdown Field (2.3 MV/cm) for GaN on Si", IEEE ELECTRON DEVICE LETTERS, VOL. 32, NO. 11, NOVEMBER 2011